Cross Sections for Electron Collisions with Acetylene

Mi-Young Song and Jung-Sik YoonHyuck ChoGrzegorz P. KarwaszViatcheslav KokoulineYoshiharu NakamuraJonathan Tennyson

Citation: Journal of Physical and Chemical Reference Data **46**, 013106 (2017); doi: 10.1063/1.4976569
View online: http://dx.doi.org/10.1063/1.4976569
View Table of Contents: http://aip.scitation.org/toc/jpr/46/1
Published by the American Institute of Physics

Cross Sections for Electron Collisions with Acetylene

Mi-Young Song[a] **and Jung-Sik Yoon**
Plasma Technology Research Center, National Fusion Research Institute, 814-2, Osikdo-dong, Gunsan, Jeollabuk-do 573-540, South Korea

Hyuck Cho
Department of Physics, Chungnam National University, Daejeon 305-764, South Korea

Grzegorz P. Karwasz
Faculty of Physics, Astronomy and Applied Informatics, University Nicolaus Copernicus, Grudziadzka 5, 87100 Toruń, Poland

Viatcheslav Kokoouline
Department of Physics, University of Central Florida, Orlando, Florida 32816, USA

Yoshiharu Nakamura
6-1-5-201 Miyazaki, Miyamae, Kawasaki 216-0033, Japan

Jonathan Tennyson
Department of Physics and Astronomy, University College London, Gower Street, London WC1E 6BT, United Kingdom

(Received 17 November 2016; accepted 2 February 2017; published online 17 March 2017)

Cross section data are compiled from the literature for electron collisions with the acetylene (HCCH) molecule. Cross sections are collected and reviewed for total scattering, elastic scattering, momentum transfer, excitations of rotational and vibrational states, dissociation, ionization, and dissociative attachment. The data derived from swarm experiments are also considered. For each of these processes, the recommended values of the cross sections are presented. The literature has been surveyed through early 2016. © *2017 AIP Publishing LLC for the National Institute of Standards and Technology.* [http://dx.doi.org/10.1063/1.4976569]

Key words: attachment; dissociation; electron collisions; evaluation; ionization; total cross sections.

CONTENTS

List of Tables

[a]Author to whom correspondence should be addressed; electronic mail: mysong@nfri.re.kr.

List of Figures

1. Introduction

Acetylene (HCCH) is the simplest triply bonded hydrocarbon molecule and has particular importance in a variety of different plasma processes. For example, plasma can be used to make HCCH from coal,[1] natural gas,[2] and methane.[3,4] Conversely acetylene plasmas are used for a variety of chemistries;[5] they are used to make C_2,[6] CH*,[7] fullerenes,[8] diamonds,[9] carbon nanoparticles,[10] hydrocarbon nanoparticles,[11] nanotubes,[12,13] and polymers,[14] as well as other chemical processes.[15,16] Acetylene plasmas are used to provide a variety of different coatings.[17,18] The role of acetylene in fusion plasmas has also been considered.[19,20] Acetylene is well-known from combustion, where oxy-acetylene flames provide particularly hot (~3000 K) flames which are in routine everyday use. Acetylene is also an important component of cool carbon-rich stars[21] whose spectra require considerable data to model.[22]

This work uses the same methodology as our recent review of electron–methane collision data.[23] However, there have been significantly fewer experimental studies of electron–acetylene collisions. This means that the accuracy for many of the cross sections we recommend is less satisfactory. Measured cross sections for processes involving ground state acetylene have been previously compiled and assessed.[24,25] In this paper, we compile and review data reported up to early 2016 for the various cross sections involving electron scattering from acetylene. We suggest recommended cross sections for the different scattering processes and identify processes which would benefit from further study.

2. Total Scattering Cross Section

The total cross section (TCS) in acetylene, compared to methane, has been measured in relatively few experiments. The TCS in the low energy region is dominated by a $^2\Pi_g$ resonant state, centered around 2.5 eV,[26] with a TCS exceeding 40×10^{-6} cm^2. At 6 eV, another $^2\Sigma_g^+$ resonant state was observed.[26] In the TCS, this latter resonance appears as a broad maximum, with a somewhat similar amplitude (about 27×10^{-16} cm^2) and position (about 8 eV) to that in CH_4, see Song *et al.*[23]

A number of theoretical studies have also characterized these resonances[27–31] generally via consideration of elastic scattering. These studies will be considered as appropriate below.

In the region of the $^2\Pi_g$ resonance, we analysed the following four experiments:

(i) absolute measurements by Brüche[32] who used a Ramsauer-type apparatus at 1–50 eV energy range;
(ii) absolute measurements with the use of an electrostatic analyzer[33] by the group of Szmytkowski *et al.*[33] at 0.6–270 eV;
(iii) absolute measurements with a magnetically guided electron (and positron) beam at 1–400 eV by Sueoka and Mori;[34]
(iv) normalized transmission current in the dissociative attachment experiment by Dressler and Allan.[35]

At high energies two experiments are available, both performed with the absolute method—by Xing *et al.*[36] and Ariyasinghe and Powers.[37]

In absolute measurements, the TCS is determined from the attenuation of the electron beam at the exit of a gas cell, i.e., from Beer-Lambert's law,

$$I = I_0 \exp(-\sigma N l), \quad (1)$$

where I is the electron current in the presence of gas in the scattering cell, I_0 is the current without gas in the scattering cell, N is the target density, and l is the gas cell length. The following sources were considered:

(i) Ramsauer's apparatus with a double scattering cell[38] which assured good angular resolution produced CH_4 total cross sections down to 0.3 eV in a very good agreement with the most recent measurements (see the work of Song *et al.* 2015). However, Brüche[39] used a single-segment scattering cell with a worse angular resolution. Brüche's paper[32] concentrates on similarities between cross sections in N_2 and C_2H_2. He reported three measurements, with two different gas samples and using "old" and "new" apparatus. Results from the new apparatus yielded a resonant maximum at a lower energy (2.3 eV) than from the old one (2.9 eV); in the final figure (Fig. 2 in Ref. 32), Brüche reported only old apparatus data, see the black line in Fig. 1. The energy scale in his measurements was determined from the geometrical electron path with the given magnetic field—any stray magnetic fields could have biased that determination.
(ii) Szmytkowski and collaborators used an apparatus with about 0.1 eV energy resolution, equipped with 30.5 mm long scattering cell and 1 msr angular resolution.[33] Reported systematic errors in C_2H_2 measurements amounted up to about 12% between 0.6 and 1.0 eV (mainly due to the electron drift and the angular resolution), 6%–9% at 1–2 eV, 4%–5% between 2 and 100 eV, and increasing again to 6%–7% at higher energies. The energy scale was determined with ±0.1 eV accuracy against the vibrational structure in the $^2\Pi_g$ resonance;[40] due to the electron drift, this determination is less precise than in some other measurements by Szmytkowski and collaborators.[33]
(iii) Sueoka and Mori[34] used secondary electrons from the radioactive source and W-moderator, a guiding magnetic field, a longer (58 mm) scattering cell but with large (8 mm diameter) apertures. The energy resolution was relatively poor, 1 eV FWHM, but the energy scale was determined intrinsically by the time-of-flight method. Measurements at 1–6 eV were performed with 3 G magnetic field and at higher energies—at 4.5 G. As shown by Karwasz *et al.*[41] in the case of a guiding magnetic field, a geometrical definition of the angular resolution does not properly characterize possible systematic errors. This is rather a "radius of gyration" smaller than exit aperture radius which should be considered: electrons scattered at lower angles are counted as non-scattered, lowering the measured TCS. Apart from the angular resolution, the remaining systematic error in the data of Sueoka and Mori was 3% and the statistical error 1.5%.
(iv) Dressler and Allan[35] used a trochoidal spectrometer with 40 meV energy resolution which was designed to determine narrow resonances in the 7.5–9.5 eV energy range. The curve of "transmitted current" was reported in the energy range from 0 to 5 eV. Unfortunately, no absolute intensity (nor zero offset) was reported. In Fig. 1, we normalized this curve to absolute TCS of Szmytkowski *et al.* at two points: 1 eV and 2.6 eV. After such a normalization, the two sets (Dressler and Allan, Szmytkowski *et al.*) agree quite well, see Fig. 1. In the previous analysis by Karwasz *et al.*,[41] the data of Dressler and Allan were used to determine the TCS below 1 eV. In that case, the data were normalized to the results of Sueoka and Mori. As a consequence, the present recommended and those from the work of

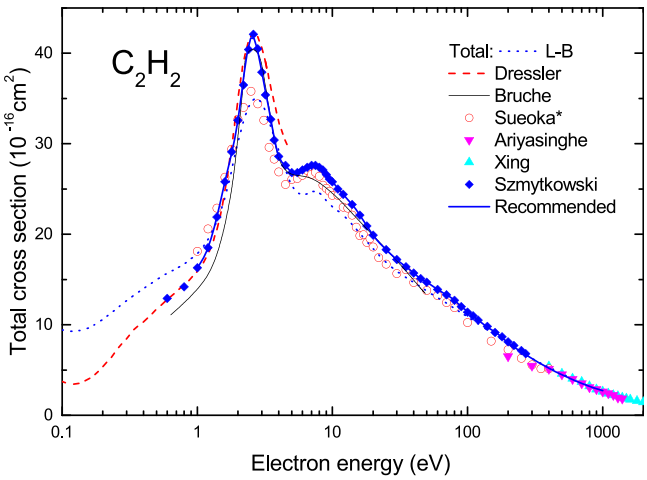

FIG. 1. Total electron-scattering cross sections in acetylene at 0.1–2000 eV. Brüche[32]—thin line, experimental points read from his Fig. 1. "Ältere Apparatur"; the absolute TCS of Sueoka and Mori[34] at 5–15 eV has been renormalized by +10% and at 16–100 eV by +5%, on the basis of a possible angular resolution error, elastic differential cross sections of Gauf *et al.*[42] have been used for this evaluation. The short broken line is the earlier set of recommended TCS,[41] based on measurements of Sueoka and Mori[34] and Dressler and Allan[35] normalized to the previous ones. Data due to Szmytkowski *et al.*,[33] Xing *et al.*,[36] and Ariyasinghe and Powers.[37]

Karwasz *et al.*[41] differ. For the 1–100 eV energy region, averaging different experiments does not seem a proper way to get recommended cross sections: Brüche's points show a big spread, the measurement of Dressler and Allan[35] is normalized in a rather arbitrary way, the TCS of Sueoka and Mori was obtained with a poor energy resolution. Instead we checked the congruence between different sets before making a recommendation.

Note that in the region of the low-energy resonance (1–5 eV) there are three sets: absolute of Brüche, absolute of Szmytkowski *et al.*, and the presently normalized of Dressler and Allan agree quite well, see Fig. 1. The TCS of Sueoka and Mori at the resonance maximum (2.5 eV) is lower (35.8×10^{-16} cm^2) than the value of Szmytkowski (42.1×10^{-16} cm^2 at 2.6 eV). However, convoluting the latter value with the 1 eV FWHM Gaussian curve would bring the maximum of 42×10^{-16} cm^2 to some 34×10^{-16} cm^2, perfectly explaining the lower value measured by Sueoka and Mori.

In the energy range above 5 eV, the TCS of Sueoka and Mori seems to be a few percent lower than that of Szmytkowski *et al.* We checked a possible angular resolution correction to the TCS of Sueoka and Mori. For 6 eV (and 4.5 G field), the gyration radius of 4 mm corresponds to the scattering angle of 13°. Using the elastic differential cross sections (DCS's) of Gauf *et al.*,[42] a missing part of the integral cross section due to scattering into 0°–13° amounts to 10%. The TCS of Sueoka and Mori at the resonance maximum (2.5 eV) is lower. For the sake of qualitative comparison, in Fig. 1 we show the TCS of Sueoka and Mori between 5 and 15 eV normalized by +10% and in-between 16–100 eV by +5%. Such corrections bring the data of Szmytkowski *et al.* and Sueoka and Mori into an agreement within declared error bars.

The TCS recommended by Karwasz *et al.*,[41] see Fig. 1, was based on experiments available at that time; it coincides with the present recommendation for 50–1000 eV; at 1–50 eV they followed the experiment by Sueoka and Mori, and as a consequence at 2–50 eV they are lower than the present recommended values by 10%–20%; below 1 eV they were based on the normalization of the relative measurements of Dressler and Allan to Sueoka and Mori and are higher than the present recommendation.

At high energies, both available experiments, Xing *et al.*[36] (covering 400–2600 eV) and Ariyasinghe and Powers,[37] covering 200–1400 eV were analyzed. Both were performed using electrostatic electron optics, and the results in the energy overlap agree within 5%. In order to extend the recommended value to 4000 eV, we used the Bethe–Born analysis, where cross sections can be approximated by the formula

$$\sigma(E) = A/E + B \log(E)/E, \qquad (2)$$

where the energy E is expressed in Rydbergs, $R = 13.6$ eV, and the cross section is expressed in atomic units $a_0^2 = 0.28 \times 10^{-16}$ cm^2. As seen from the figure, selected points of TCS can be roughly approximated by a straight-line: with $A = -70$ and $B = 420$ in the given units. However, this fit is rather arbitrary, with some ±15% uncertainty, due to the poor quality of experiments in their high energy limits, where the angular resolution errors tend to underestimate TCS, see Fig. 2. The overall uncertainty on the recommended TCS in the 2–200 eV range is ±10%. Below 2 eV and above 200 eV, this uncertainty rises to 15%. Resuming, the present recommended TCS follows experimental results by Szmytkowski *et al.*[33] in the energy range 1–170 eV, using interpolated values for some energy points, and is derived from the Bethe-Born fit, Eq. (2), at 200–1000 eV. The overall uncertainty on the recommended TCS in 2–200 eV is 10%. Below 2 eV and above 200 eV, this uncertainty rises to 15%. Recommended values of TCS with their uncertainties are given in Table 1.

3. Elastic Scattering Cross Section

There have been only a few experimental investigations of elastic electron scattering from acetylene. After excluding those publications reporting the relative measurements and/or the cross sections with no uncertainties, only four reports relevant to this evaluation are available. These are Khakoo *et al.*,[43] Iga *et al.*,[44,45] and Gauf *et al.*[42] However, the results of Khakoo *et al.*[43] were superseded by the new measurements of Gauf *et al.*[42] which are also from Khakoo's group. Therefore, in this evaluation, we considered only Iga *et al.*[44,45] and Gauf *et al.*[42] Iga *et al.* reported experimental absolute elastic cross sections at nine electron energies in the (50–500 eV) energy range, and Gauf *et al.*[42] at 13 electron energies in the (1–100 eV) energy range. The two sets of cross sections agree with each other fairly well at the energies (50, 80, and 100 eV) where they overlap. Therefore, we assume that the agreement assures the reliability of the cross section even in the low-energy region (below 50 eV) and high-energy region (above 100 eV) where there is only a single set of cross sections for each electron energy. For electron energies 50, 80, and 100 eV, we averaged two cross section sets from Iga *et al.*[44,45] and Gauf *et al.*[42] and

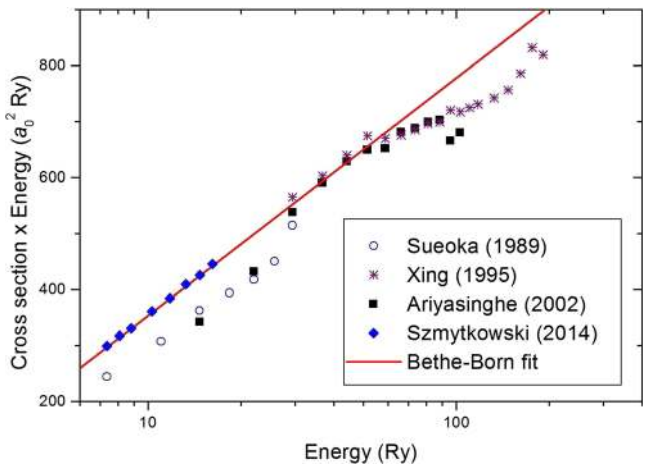

FIG. 2. Total electron-scattering cross sections in acetylene in the high energy limit: Born–Bethe plot, see text for explanations. The approximate linear plot is based on the points of Szmytkowski *et al.*[33] in the 120–270 eV energy range, and Xing *et al.*[36] and Ariyasinghe and Powers[37] points at 400–800 eV. Note that TCS measurements can easily be underestimated at high energies.

TABLE 1. Recommended total cross sections for electron scattering in acetylene (in 10^{-16} cm^2 units). Data in the energy ranges 1–170 and 200–1000 eV have been obtained with complementary procedures, see text for explanations

Energy	TCS	δ	Energy	TCS	δ
1.0	16.3	2.4	40	15.7	1.6
1.2	18.5	2.8	45	15.1	1.5
1.5	23.9	3.6	50	14.7	1.5
1.7	27.5	4.1	60	13.9	1.4
2.0	32.6	3.3	70	13.3	1.3
2.5	41.7	4.2	80	12.7	1.3
3.0	37.9	3.8	90	12.0	1.2
3.5	32.7	3.3	100	11.5	1.2
4.0	28.6	2.9	120	10.5	1.1
4.5	27.6	2.8	150	9.5	0.9
5.0	26.8	2.7	170	8.9	0.9
6.0	27.1	2.7	200	8.0	0.8
7.0	27.6	2.8	250	7.0	1.0
8.0	27.4	2.7	300	6.3	0.9
9.0	26.6	2.7	350	5.7	0.9
10	25.8	2.6	400	5.2	0.8
12	24.4	2.4	450	4.8	0.7
15	22.7	2.3	500	4.5	0.7
17	21.5	2.2	600	3.9	0.6
20	19.9	2.0	700	3.5	0.5
25	18.3	1.8	800	3.2	0.5
30	17.2	1.7	900	2.9	0.4
35	16.4	1.6	1000	2.7	0.4

derived the recommended elastic differential and integral cross sections and the associated uncertainties. For other electron energies, we just recommended the original cross sections and the uncertainties of Iga *et al.*[44,45] and Gauf *et al.*[42] Complete numerical values for elastic differential cross sections (DCS's) are presented in Table 2, and the figures for six representative energies are in Fig. 3. Similarly, the recommended integral cross sections (ICS's) are presented in both tabulated and graphic form, respectively, in Table 3 and Fig. 4. The methods used to integrate the DCS's to obtain ICS's vary slightly between authors and, therefore, it is necessary to refer to the original paper for the particular method employed.

4. Momentum Transfer Cross Section

The momentum-transfer cross section for electron–acetylene collision has been determined in several recent studies in which elastic differential cross sections were measured or calculated and also in a recent electron swarm study in which a set of electron collision cross sections for acetylene including the momentum transfer and vibrational cross sections (see Sec. 6) are simultaneously determined in order to be consistent with all experimental swarm data measured both in pure C_2H_2 and in C_2H_2–Ar mixtures simultaneously. The data presented by Gauf *et al.*[42] agree very well with a previous experimental work by Iga *et al.*[44] and they also agree with the result of the electron swarm study within combined uncertainty limits of these studies over the energy ranges overlap. Therefore, those three sets of experimental momentum-transfer cross sections are equally recommended here to cover the energy range from 0.1 to 500 eV with their claimed uncertainties. Theoretical cross sections determined in the work by Gauf *et al.*,[42] and also by Jain[46] and Gianturco and Stoecklin[28] agree with each other within 5%–10% above 1 eV.

However, they are larger than the experimental data by about 20% over the whole 1–10 eV interval, where the experimental data are available. The disagreement is larger near the resonance at energies 1.5–3 eV.

Figure 5 and Table 4 show the data from several previous theoretical and experimental studies.

5. Rotational Excitation Cross Section

The rotational constant B_0 of HCCH is 1.176 654 32 cm^{-1}.[47] The molecule does not have a permanent dipole moment. Its quadrupole moment is 4.856 $e\,a_0^2$.[48] Therefore, inelastic rotational transitions $j \to j'$ are allowed only for $\Delta j = |j' - j| \geq 2$. The only data available for the rotational excitation of HCCH are from the theoretical study by Thirumalai, Onda, and Truhlar,[49] where differential cross sections for the $j = 0 \to j' = 0, 2, 4, 6, 8$ transitions are reported for a single scattering energy of 10 eV. The data are shown in Fig. 6.

6. Vibrational Excitation Cross Sections

The acetylene molecule has five vibrational modes, two of which are doubly degenerate. The modes and the corresponding vibrational energies are listed in Table 5.

There are not much data on the vibrational excitation of HCCH. The only available theoretical data are for the excitation of the υ_2-mode via the $^2\Pi_g$ electronic resonance of $HCCH^-$.[27] The resonance energy and width were computed using a multi-reference configuration-interaction approach with single and double excitations with a basis set of Cartesian Gaussian-type orbitals (GTOs). The energy and the width of the resonance were determined for several values of the C–C distance. The cross section for the excitation of the C–C bond, which should approximately be equal to the v_2-mode excitation cross section, is then evaluated using the boomerang approximation.[27]

There are two beam experiments by Kochem *et al.*[50] and Khakoo *et al.*[43] and one swarm study by Nakamura,[25] in which cross sections for the excitation of different vibrational modes have been determined. Because the excitation energies of the υ_1 and υ_3 modes as well as energies of υ_4 and υ_5 modes are similar, in the swarm study υ_1/υ_3 and υ_4/υ_5 are assumed to be unresolved. The experimental data for the υ_1/υ_3, υ_4/υ_5, and υ_2 modes and for the excitation of two quanta $\upsilon_4 + \upsilon_5$ are shown in Fig. 7. As one can see, the data obtained from the swarm experiment agree well with the beam experiments for the υ_2 and υ_4/υ_5 modes as well as for $\upsilon_4 + \upsilon_5$ excitation. For the υ_1/υ_3 mode, the swarm data agree well with the experiment by Kochem *et al.*[50] but the agreement is less satisfactory with the later experiment by Khakoo *et al.*[43]

The recommended cross sections are the data from the swarm experiments by Nakamura (see Table 6).[25]

TABLE 2. Recommended elastic electron-scattering DCS's from acetylene. DCS and δ indicate cross sections and uncertainties, respectively, in units of 10^{-16} cm^2 sr^{-1}

Angle	1.0 eV DCS	δ	1.5 eV DCS	δ	2.0 eV DCS	δ	2.5 eV DCS	δ	3.0 eV DCS	δ
15									7.1	0.8
20	2.3	0.3	2.7	0.2	4.1	0.4	8.5	0.8	6.1	0.6
25	1.73	0.18	1.89	0.17	3.4	0.3	6.04	0.59	5.62	0.58
30	1.28	0.14	1.87	0.19	3.33	0.3	5.55	0.53	5.15	0.65
40	1.15	0.11	1.66	0.16	2.43	0.21	3.56	0.33	3.79	0.35
50	1.09	0.1	1.51	0.13	2.33	0.21	3.08	0.28	2.8	0.28
60										
70	1.43	0.13	1.94	0.17	2.66	0.24	2.57	0.23	1.81	0.17
80	1.46	0.17	2.14	0.19	2.76	0.2	2.3	0.21	1.76	0.17
90	1.45	0.13	2.02	0.17	2.37	0.21	2.17	0.19	1.55	0.15
100										
110	1.37	0.12	1.32	0.12	1.25	0.13	1.25	0.12	1.16	0.11
120										
130	1.07	0.1	0.68	0.06	0.96	0.09	1.52	0.14	2.16	0.21

Angle	5 eV DCS	δ	10 eV DCS	δ	15 eV DCS	δ	20 eV DCS	δ	30 eV DCS	δ
5									20	1.6
10			12.3	1.3	13.3	1.4	17.7	1.7	13.8	1.5
15	5.9	0.7	10.2	1	9.7	1.1	12.1	1.1	8.4	0.9
20	5.2	0.6	6.6	0.6	7.1	0.8	8.34	0.78	5.11	0.53
25	5.18	0.6	5.2	0.47	5.41	0.52	5.38	0.5	3.14	0.32
30	4.52	0.46	4.48	0.41	4.12	0.37	3.58	0.33	1.97	0.21
40	3.56	0.37	2.79	0.25	2.17	0.2	1.65	0.15	0.9	0.09
50	2.44	0.21	1.87	0.17	1.26	0.11	0.88	0.08	0.44	0.05
60										
70	1.27	0.11	0.93	0.08	0.65	0.06	0.38	0.03	0.21	0.02
80	1.01	0.1	0.88	0.08	0.6	0.05	0.36	0.03	0.18	0.02
90	0.96	0.09	0.85	0.07	0.58	0.05	0.36	0.03	0.18	0.02
100										
110	1.29	0.11	0.82	0.08	0.63	0.06	0.37	0.03	0.21	0.02
120										
130	1.52	0.14	0.92	0.08	0.73	0.06	0.52	0.05	0.34	0.03

Angle	50 eV DCS	δ	80 eV DCS	δ	100 eV DCS	δ	150 eV DCS	δ	200 eV DCS	δ
8							15.5	1.7	12.8	1.4
10	15.44	3.77	14.23	2.49	10.11	2.49	9.59	1.05	8.45	0.93
15	7.92	2.37	7.12	1.28	5.04	1.28	4.9	0.54	3.41	0.38
20	4.14	1.23	3.17	0.79	2.27	0.79	2.02	0.22	1.55	0.17
25										
30	1.25	0.38	0.83	0.22	0.6	0.22	0.552	0.061	0.414	0.046
40	0.48	0.13	0.34	0.07	0.27	0.07	0.266	0.029	0.235	0.026
50	0.24	0.04	0.18	0.03	0.17	0.03	0.175	0.019	0.151	0.017
60							0.115	0.013	0.0815	0.009
70	0.13	0.02	0.09	0.02	0.09	0.02	0.078 5	0.008 6	0.0542	0.006
80	0.11	0.02	0.08	0.01	0.07	0.01	0.059 8	0.006 6	0.0397	0.0044
90	0.11	0.02	0.08	0.02	0.08	0.02	0.050 1	0.005 5	0.0364	0.004
100							0.053 5	0.005 9	0.0336	0.0037
110	0.15	0.03	0.1	0.02	0.08	0.02	0.052 9	0.005 8	0.0329	0.0036
120							0.061 2	0.006 7	0.0329	0.0036
130	0.26	0.26	0.16	0.04	0.1	0.04	0.068 8	0.007 6	0.0331	0.0036

Angle	300 eV DCS	δ	400 eV DCS	δ	500 eV DCS	δ	1000 eV DCS	δ
5							15.7	1.7
8	10.9	1.2	8.26	0.91	6.41	0.71		
10	6.92	0.76	4.83	0.53	3.86	0.42	2.38	0.26
15	2.74	0.3	1.85	0.2	1.27	0.14	0.912	0.1
20	1.14	0.13	0.737	0.081	0.607	0.067	0.545	0.06
25								
30	0.394	0.043	0.321	0.035	0.288	0.032	0.112	0.012
40	0.234	0.026	0.142	0.016	0.103	0.011	0.049 3	0.005 4
50	0.114	0.013	0.0631	0.006 9	0.0497	0.005 5	0.020 2	0.002 2
60	0.0602	0.0066	0.0384	0.004 2	0.0336	0.003 7	0.012 1	0.001 3
70	0.0441	0.0049	0.0253	0.002 8	0.0201	0.002 2	0.006 72	0.000 74
80	0.0359	0.0039	0.0177	0.001 9	0.0131	0.001 4	0.004 6	0.000 51

TABLE 2. Recommended elastic electron-scattering DCS's from acetylene. DCS and δ indicate cross sections and uncertainties, respectively, in units of 10^{-16} cm^2 sr^{-1}—Continued

Angle	300 eV DCS	δ	400 eV DCS	δ	500 eV DCS	δ	1000 eV DCS	δ
90	0.0288	0.0032	0.0126	0.001 4	0.0106	0.001 2	0.003 61	0.000 4
100	0.0212	0.0023	0.0117	0.001 3	0.0087	0.000 96	0.002 56	0.000 28
110	0.0198	0.0022	0.0091	0.001	0.0074	0.000 81	0.002 39	0.000 26
120	0.02	0.0022	0.0082	0.000 9	0.0062	0.000 68	0.002 01	0.000 22
130	0.02	0.0022	0.0072	0.000 79	0.006	0.000 66	0.001 58	0.000 17

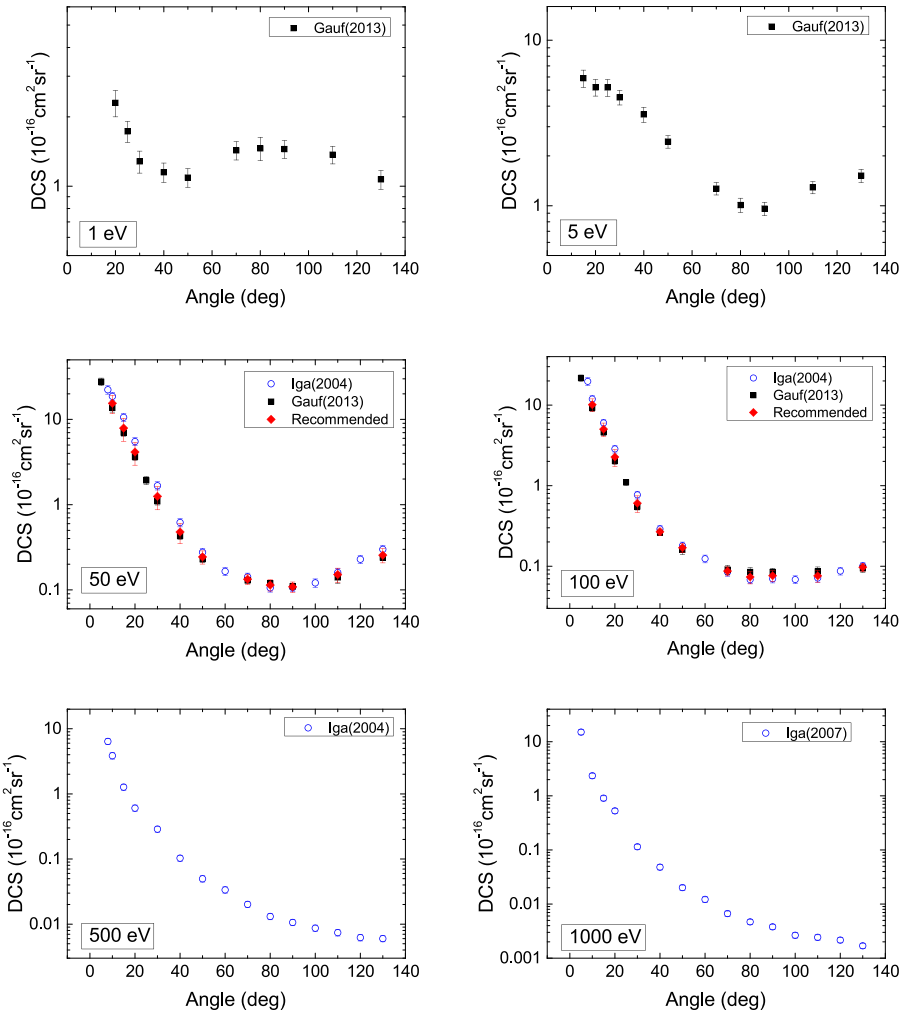

FIG. 3. Recommended elastic-scattering differential cross sections with the selected sets of data from the publications of Iga *et al.*[44,45] and Gauf *et al.*[42] For Iga's data, the uncertainty is mostly hidden by the circular symbols.

7. Electronic Excitation Cross Section

Due to the highly reactive character of the radicals formed following the dissociation of C_2H_2, few experiments have been performed on electronic excitation; furthermore, we are not aware of measurements of dissociation cross sections. Electron energy loss spectra at forward scattering (0° and 10° angles) and energies 40 and 50 eV (Ref. 51) showed that the excitation into the second lowest singlet state ($\tilde{B}\,^1B_u \leftarrow \tilde{X}\,^1\Sigma_g^+$) is by a factor of about 20 lower than to the $\tilde{C}\,^1\Pi_u$ state; excitation to the lowest excited singlet state, $\tilde{A}\,^1A_u$, was under the detection threshold in that experiment. Electronic excitations to both singlet and triplet states at 25 and 35 eV electron collision energies and in the 10°–80° scattering angles range were studied by Trajmar *et al.*[52,53] DCS for the $\tilde{C}$ (8.16 eV energy loss for $\nu_2' = 0$) and the $\tilde{D}$ (9.26 eV energy loss for $\nu_2' = 0$) states are both of similar intensity at 25 and 35 eV; the $\tilde{C}$ state is slightly more forward-centered. At 10°, the maximum in the DCS for a broad $\tilde{B}$, 7.2 eV energy-loss band is by a factor of 20 lower than the maxima for $\tilde{C}$ and

TABLE 3. Recommended elastic ICS's for acetylene. ICS and δ are given in units of 10^{-16} cm^2

Energy	ICS	δ
1.0	16.80	3.30
1.5	19.30	3.40
2.0	25.30	4.50
2.5	33.10	5.90
3.0	30.10	5.90
5.0	24.00	4.80
10	20.60	3.80
15	17.20	3.30
20	15.20	2.80
30	9.70	2.00
50	8.30	2.30
80	6.85	1.58
100	5.08	1.33
150	4.72	1.47
200	3.78	1.18
300	3.17	0.99
400	2.33	0.72
500	1.81	0.56
1000	1.43	0.44

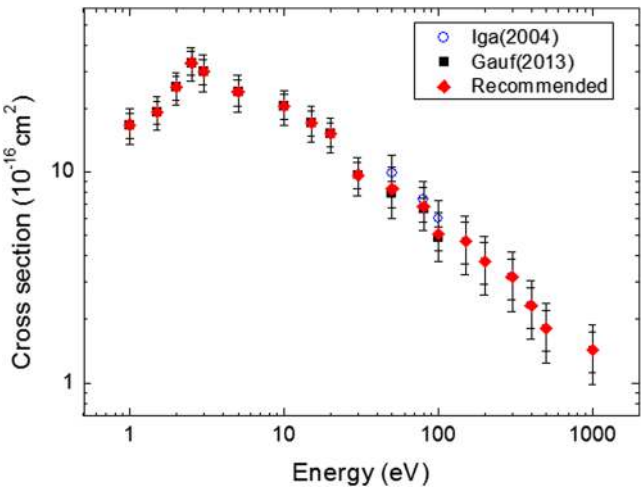

FIG. 4. Recommended elastic integral cross sections with the selected sets of data from Iga *et al.*[44,45] and Gauf *et al.*[42]

$\tilde{D}$ excitations; at 50°, the maxima for excitation into $\tilde{a}$, $\tilde{b}$, $\tilde{A}$, $\tilde{B}$, $\tilde{C}$, and $\tilde{D}$ states scale as 0.5, 0.7, 1.0, 4, and 8, respectively[52] (we adopt the state notation given in the original paper).

DCS's for $\tilde{a}\,^3A_u$ and $\tilde{b}\,^3B_u$ (5.2 and 6.1 eV energy loss, respectively) triplet states rise between 10° and 80° scattering angles. At 70° (and 25 eV collision energy), DCS's for excitation into these three states is of similar amplitude, being a factor of 5 lower than the excitation into the $\tilde{C}$ state and by a factor of 10 lower than the excitation into the $\tilde{D}$ state.[52] Between 25 and 35 eV collision energies, relative values for all these states increase roughly by a factor of two, apart from the $\tilde{a}$-state which rises by a factor of four.[53]

Studies of electron scattering at zero angle (i.e., corresponding to the photo-absorption) done with 1 eV energy resolution showed two peaks in the oscillator strength: of 0.45 at 9.5 eV and 0.51 at 15.5 eV.[54] We recall this reference for the detailed assignment of the excited states and comparison of vibronic oscillator strengths.

A rough evaluation of the overall integral excitation cross section can be made from the difference between total and elastic (plus ionization above the threshold) cross sections. This difference, using our recommended integral cross sections, amounts to 1.1×10^{-16} cm^2 at 5 eV, rising to 2.4×10^{-16} cm^2 at 10 eV and falling to 1.5×10^{-16} cm^2 at 30 eV. Note, however, that uncertainty bars both on elastic and total cross sections are of the same order of magnitude as these values.

Finally, we note that Vinodkumar *et al.*[31] present some calculated electronic excitation cross sections. However, these calculations provide no indication of uncertainties so it is difficult to use them as the basis for a recommendation.

8. Ionization Cross Section

Recommended total and partial ionization cross sections from Landolt-Börnstein compilation[55] were based exclusively on recent time-of-flight measurements by Tian and Vidal[56] up to 600 eV electron impact energy. The data were normalized to the Ar^+ cross section of Straub *et al.*[57] The uncertainty in these cross section is on the order of $\pm 10\%$, if the magnitude of the cross section is greater than 1×10^{-17} cm^2, otherwise it is on the order of $\pm 15\%$.[55]

The present analysis takes into account all the data available to us, starting from early measurements by Tate and Smith.[58] Recommended values are given in Table 7 and the detailed analysis of data follows.

8.1. Total ionization cross section

Total ionization cross sections from different experiments are compared in Fig. 8. Apart from Tian and Vidal,[56] another recent measurement of the absolute ionization cross sections is that by Zheng and Srivastava[59] which extends up to 800 eV. Total (and partial) ionization cross sections were measured with a quadrupole and with a time-of-flight spectrometer. The "ionization efficiencies" have been normalized using ionization cross sections in H_2, N_2, and Ne, via a relative flow technique; the declared accuracy of the cross sections is $\pm 13\%$. The total cross sections of Zheng and Srivastava in the 40–600 eV energy range are some 10% lower than those of Tian and Vidal[56] but higher by a similar amount at 20 eV.

Earlier absolute measurements of total ionization cross sections include those by Tate and Smith[58] up to 750 eV, Gaudin and Hagemann[62] at energies between 100 and 900 eV, Azria and Fiquet-Fayard[63] up to 100 eV, and Durić *et al.*[64] up to 200 eV. The latter measurements have been extended up to 1000 eV by Josifov *et al.*[60]

Experiments by Tate and Smith,[58] Azria and Fiquet-Fayard,[63] Durić *et al.*,[64] and Josifov *et al.*[60] used scattering cells with well defined lengths, so, in principle, they should provide a better accuracy on total cross sections than experiments using crossed beams.[56,59] Apart from the data by

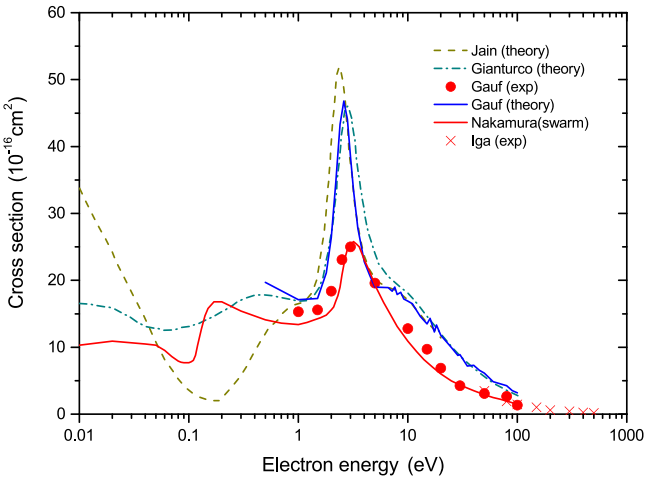

FIG. 5. Momentum-transfer cross sections for elastic collisions of acetylene with electrons obtained in different studies. The recommended data (Iga *et al.*,[44] crosses; Nakamura,[25] thick solid line; and Gauf *et al.*,[42] solid circles) are shown by red symbols. The thin solid, dashed, and dotted–dashed lines represent theoretical calculations by Gauf *et al.*,[42] Jain,[46] and Gianturco and Stoecklin,[28] respectively.

TABLE 4. Recommended momentum transfer cross sections in units of 10^{-16} cm^2

Energy	Iga *et al.*[44]	Nakamura[25]	Gauf *et al.*[42]
0.00	...	10.2	...
0.01	...	10.3	...
0.02	...	10.9	...
0.05	...	10.3	...
0.06	...	9.52	...
0.08	...	7.93	...
0.10	...	7.70	...
0.11	...	8.04	...
0.12	...	10.3	...
0.14	...	14.7	...
0.17	...	16.8	...
0.20	...	16.8	...
0.30	...	15.4	...
0.50	...	14.1	...
0.70	...	13.6	...
1.0	...	13.4	15.3
1.4	...	14.1	...
1.5	...	...	15.6
1.8	...	14.8	...
2.0	...	15.6	18.4
2.5	...	20.8	23.1
3.0	...	25.4	25.0
3.2	...	25.8	...
3.6	...	25.0	...
4.0	...	23.1	...
5.0	...	19.3	19.6
7.0	...	14.8	...
10.0	...	10.9	12.8
14.0	...	8.15	...
15.0	...	...	9.7
20.0	...	6.01	6.86
30.0	...	4.37	4.24
50.0	3.46	2.92	3.08
70.0	...	2.23	...
80.0	1.92	1.95	2.67
100	1.44	1.50	1.34
150	1.02	...	...
200	0.617	...	...
300	0.443	...	...
400	0.237	...	...
500	0.188	...	...

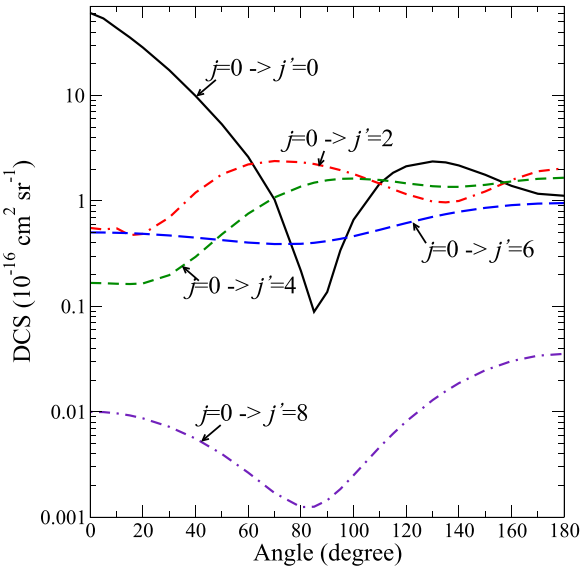

FIG. 6. Differential cross sections for rotational excitation $j = 0 \rightarrow j' = 0, 2, 4, 6, 8$ of HCCH in collisions with electrons due to Thirumalai, Onda, and Truhlar.[49] The scattering energy is 10 eV.

TABLE 5. Vibrational modes and excitation energies for HCCH[47]

	Mode	Energy (eV)
ν_1	Symmetric C–H stretch, σ_g^+	0.421 189
ν_2	Symmetric C–C stretch, σ_g^+	0.245 712
ν_3	Asymmetric C–H stretch, σ_u^+	0.411 238
ν_4	Symmetric bend, π_g	0.075 472 9
ν_5	Asymmetric bend, π_u	0.090 394 4

Gaudin and Hagemann,[62] all earlier experiments[58,63,64] are only slightly (less than 5%) lower than those by Zheng and Srivastava.[59] Data by Gaudin and Hagemann are lower by 20%–30% than all other sets—probably due to an incomplete collection of light ions. Data by Josifov *et al.*[60] seem to be affected in a similar way in their high-energy limit, see Fig. 8.

Different experimental determinations of the total ionization cross section in acetylene show bigger discrepancies than is observed, for example, in methane, see Song *et al.*[23] Extensive description of calibration and normalization procedures was given only by Zheng and Srivastava[59] and Tian and Vidal.[56] These two experiments agree within the combined declared uncertainties (13% and 10%, respectively). Therefore, for the recommended total cross sections, we used only these two sets; both of them were interpolated by cubic splines with 1 eV steps and average (not weighted) values were calculated. The recommended values are given in Table 7. The uncertainty on the total ionization cross sections in the range 22.5–600 eV on these points is ±8%.

Data of Tian and Vidal in their low-energy limit are significantly (almost 50% at 17.5 eV) lower than all other experiments. Therefore, in 15–20 eV, the average values between Josifov *et al.*[60] and Tate and Smith[58] are recommended, see Table 7. The uncertainty on these points is ±10%.

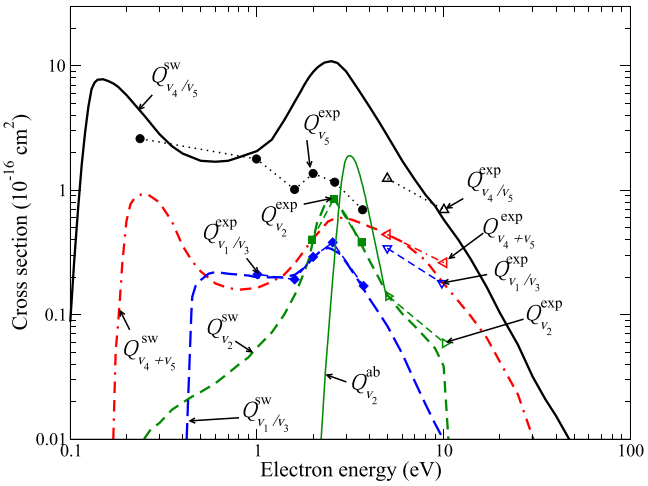

FIG. 7. Summary of data for vibrational excitation cross sections in e^-–HCCH collisions. Thick lines without symbols (Q^{sw}) are the data from swarm experiments by Nakamura,[25] open symbols are the data from the experiment by Khakoo *et al.*,[43] and full symbols are the data from the experiment by Kochem *et al.*[50] The solid thin green line ($Q^{ab}_{\nu_2}$) is the *ab initio* results by Krumbach, Nestmann, and Peyerimhoff.[27]

TABLE 6. Recommended vibrational excitation cross sections in units of 10^{-16} cm^2

Energy	σ_{ν_4/ν_5}	Energy	$\sigma_{\nu_4+\nu_5}$	Energy	σ_{ν_2}	Energy	σ_{ν_1/ν_3}
0.09	0	0.166	0	0.246	0	0.411	0
0.10	0.0885	0.19	0.260	0.30	0.0135	0.45	0.139
0.12	2.90	0.20	0.566	0.50	0.0239	0.47	0.172
0.13	6.50	0.21	0.771	0.70	0.0338	0.50	0.190
0.14	7.71	0.22	0.855	1.0	0.0544	0.55	0.213
0.15	7.78	0.24	0.924	1.4	0.100	0.60	0.220
0.17	7.20	0.26	0.924	1.7	0.181	0.80	0.210
0.20	5.81	0.30	0.798	2.0	0.398	1.0	0.200
0.25	3.95	0.35	0.561	2.2	0.641	1.2	0.200
0.30	2.82	0.40	0.356	2.3	0.756	1.4	0.200
0.40	1.97	0.50	0.222	2.4	0.835	1.6	0.210
0.70	1.72	0.60	0.178	2.5	0.848	1.8	0.239
1.0	2.06	0.80	0.158	2.6	0.835	2.0	0.287
1.2	2.55	1.0	0.164	2.7	0.781	2.2	0.327
1.4	3.65	1.2	0.184	2.8	0.720	2.4	0.343
1.6	5.20	1.4	0.210	3.0	0.621	2.6	0.327
2.0	8.93	1.8	0.330	3.5	0.405	3.0	0.264
2.2	10.2	2.0	0.410	4.0	0.273	4.0	0.134
2.5	10.9	2.4	0.560	5.0	0.144	5.0	0.0808
2.7	10.5	2.6	0.590	7.0	0.0405	7.0	0.0291
3.0	9.00	2.8	0.600	10	0.0000	10	0.0000
3.5	6.39	3.0	0.590				
4.0	4.69	4.0	0.510				
5.0	2.73	6.0	0.385				
7.0	1.22	10	0.178				
10	0.581	20	0.0418				
20	0.103	30	0.0000				
50	0.000						

8.2. Partial ionization cross sections

In contrast to CH_4, the parent ion $C_2H_2^+$ channel in the 50–800 eV energy range amounts to about 2/3 of the total ionization cross section.[56] In the same energy range, the CH_2^+ ion is formed roughly in 15% of ionization events, see Fig. 9. The cross section for H^+ production in its maximum (100 eV) is 8% of the total ionization, see Fig. 9.

TABLE 7. Total and partial ionization cross sections for electron collisions on acetylene (in 10^{-16} cm^2 units). Total cross sections were obtained as non-weighted averages of the absolute values by Zheng and Srivastava[59] and Tian and Vidal,[56] apart from the energies below 15–20 eV, where they are the average of the absolute values of Tate and Smith[58] and Josifov *et al.*[60] Partial cross sections are non-weighted averages between the absolute values of Zheng and Srivastava,[59] Tian and Vidal,[56] and normalized values of Feil *et al.*,[61] apart from H^+ where only two sets were used (no data are reported by Feil *et al.*)

Energy (eV)	$C_2H_2^+$	C_2H^+	CH^+	C_2^+	C^+	H^+	Total
15.0	0.710						0.71
17.5	1.350						1.35
20.0	1.670	0.130					1.80
22.5	2.060	0.274				0.008	2.30
25	2.454	0.400	0.013	0.024	0.0002	0.025	2.89
30	2.850	0.571	0.062	0.097	0.017	0.063	3.65
35	3.082	0.662	0.106	0.149	0.036	0.113	4.12
40	3.226	0.706	0.149	0.180	0.060	0.175	4.45
45	3.317	0.742	0.191	0.198	0.080	0.234	4.69
50	3.410	0.764	0.230	0.211	0.095	0.287	4.92
60	3.487	0.787	0.285	0.223	0.114	0.355	5.16
70	3.521	0.793	0.317	0.228	0.127	0.397	5.28
80	3.567	0.790	0.338	0.229	0.137	0.421	5.38
90	3.565	0.784	0.345	0.230	0.144	0.432	5.41
100	3.496	0.762	0.342	0.224	0.144	0.432	5.32
110	3.412	0.744	0.335	0.218	0.142	0.425	5.20
125	3.314	0.728	0.322	0.210	0.138	0.408	5.06
150	3.171	0.703	0.303	0.196	0.132	0.380	4.82
175	3.022	0.671	0.282	0.183	0.122	0.350	4.56
200	2.904	0.641	0.263	0.171	0.114	0.321	4.35
250	2.632	0.581	0.228	0.149	0.097	0.272	3.90
300	2.393	0.522	0.198	0.131	0.082	0.232	3.50
400	2.019	0.436	0.153	0.105	0.062	0.176	2.90
500	1.771	0.375	0.124	0.087	0.051	0.147	2.50
600	1.565	0.329	0.103	0.073	0.042	0.118	2.18
Uncertainty (%)	8[a]	15	20	15	40	15	8–10

[a]10% at 15–20 eV.

In detail, cross sections for the formation of specific ions were measured by Tate *et al.*,[65] Gaudin and Hagemann,[62] Zheng and Srivastava[59] (with a time-of-flight spectrometer for H^+ ion and a quadrupole spectrometer for all other ions), Tian and Vidal,[56] Feil *et al.*,[61] and King and Price.[66] Josifov *et al.*[60] reported ionization into $C_2H_2^+$ and the sum of dissociative ionization cross sections. Feil *et al.*[61] measured partial cross sections using a tandem of magnetic- and electric-field spectrometer which allowed them to determine also kinetic energies of fragment ions. Their partial cross sections were normalized to the sum of $C_2H_2^+$, C_2H^+, C_2^+, C^+, and CH^+ absolute cross sections of Tian and Vidal.[56] Feil *et al.*[61] did not report H^+ ions as they were difficult to distinguish with their spectrometer. King and Price,[66] using coincidence maps, measured the signal of dissociated ionic fragments coming from single, double, and triple ionization processes. They normalized their partial cross sections to the $C_2H_2^+$ cross section of Tian and Vidal.[56] Therefore, any systematic error in the absolute values of Tian and Vidal can propagate to both the data of Feil *et al.*[61] and King and Price.[66] Three recent sets of partial cross sections[56,59,61] agree very well (within ±5%) for the main ionization channels ($C_2H_2^+$), within ±10% for C_2H^+, within 20% for CH^+ and C_2^+, for all ions; the data of Zheng and Srivastava[59] are the lowest. The agreements are

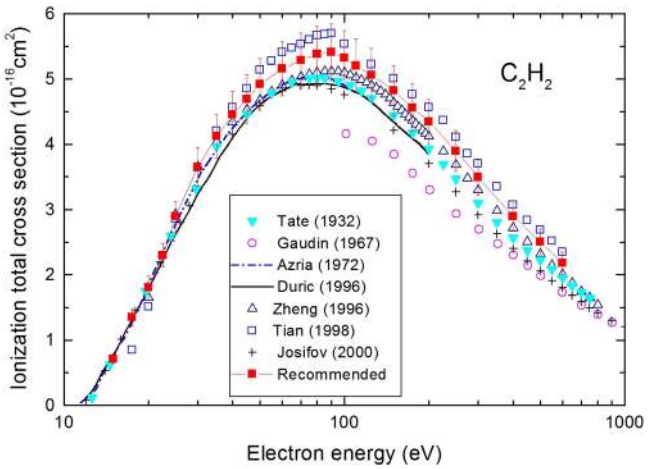

FIG. 8. Total (gross) ionization cross sections in acetylene—experimental data: Tate and Smith,[58] inverted triangle; Gaudin and Hagemann,[62] circles; Azria and Fiquet-Fayard,[63] dashed–dotted line; Durić *et al.*,[64] solid line; Zheng and Srivastava,[59] triangles; Tian and Vidal,[56] open squares; Josifov *et al.*,[60] crosses. Data of Azria and Fiquet-Fayard[63] and Durić *et al.*[64] have been read from figures. Recommended values are not-weighted average over Zheng and Srivastava[59] and Tian and Vidal[56] (±8% uncertainty) from 25 to 600 eV and Josifov *et al.*[60] and Tate and Smith[58] (±10% uncertainty) at 15–22.5 eV.

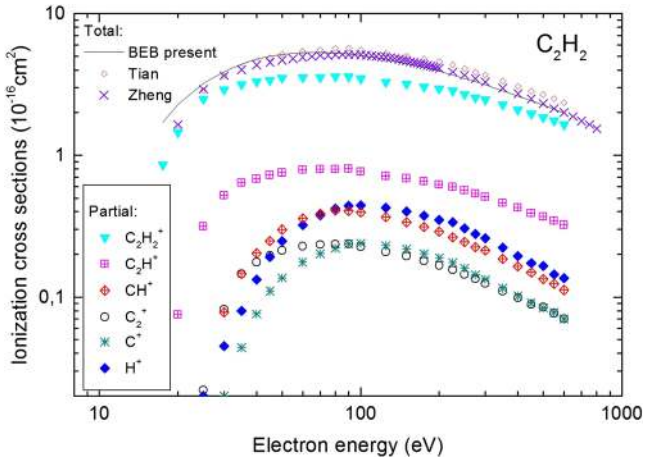

FIG. 9. Comparison between gross total and partial ionization cross sections. Total and partial cross sections are experimental data by Tian and Vidal.[56] The present BEB model and total cross sections of Zheng and Srivastava[59] are drawn for comparison.

quite poor for the C^+ ion (which is not resolved from C_2^{2+} ion)—a discrepancy by a factor of 2 between Feil *et al.* and Tian and Vidal, see Fig. 10. Earlier measurements[62,65] for heavier ions agree reasonably well with Zheng and Srivastava (within 10% for $C_2H_2^+$, 20% for C_2H^+ and C_2^+) but poorly for light ions (discrepancy of a factor of 2 for CH^+ and C^+), with older measurements being lower. Recommended values are calculated as non-weighted averages between absolute values of Zheng and Srivastava,[59] Tian and Vidal,[56] and normalized (to the latter) values of Feil *et al.* For the H^+ ion, only the data of Zheng and Srivastava[59] and Tian and Vidal[56] were used. (Note an energy shift in two sets, Fig. 10, probably due to different energy determinations in the two different spectrometers used.) In the energy region 15–20 eV present, recommended total values (at 20 eV with CH_2^+ signal subtracted) were used as $C_2H_2^+$ recommended values. The uncertainty limits on the recommended values were evaluated from the spread between average values and single experimental sets. Note that for recommended total and recommended partial cross sections, the averaging procedures were applied on different experiments (two for total and three for partial). Therefore, it would be justified if the summed partial cross sections were different from total; in fact, the summed cross sections are higher, but the difference is as little as 1%–2%, so within uncertainty bar total cross sections.

8.3. Double and triple ionization

Analysis of two-ion events can be made using the data of King and Price[66] (Fig. 11). Single ionization into C_2H^+ shows a similar energy dependence as $C_2H_2^+$. A second group of partial cross sections with similar energy dependencies is single ionization events yielding CH^+ or H^+. Double-ion events show similar energy dependencies that are H^+ (dominating), CH^+, and C_2H^+ ions. The cross section for the formation of H^+ ions is peculiar: above 100 eV, the contribution to the formation of this ion via double ionization events is greater (and amounts to 0.18×10^{-16} cm^2) than from single ionization. At 200 eV, the H^+ ion is produced in 68% of double ionization events.[66]

A second group of fragment ions appearing from dissociation of doubly charged ions, with a higher threshold, is C^{2+} and C^+ ions, see Fig. 11. In contrast to earlier measurements, King and Price reported also CH_2^+ ions, with intensity at 200 eV more than two orders of magnitude lower than that of C_2H^+ and doubly charged C^{2+} ions, with three orders of magnitude difference at 200 eV, see Fig. 11. Cross sections for triple ionization are, roughly, two orders of magnitude lower than from double ionization. For example, at 200 eV, the cross section for the formation of H^+ ion via triply charged ions amounts to 0.24×10^{-18} cm^2 while that of C^+ to 0.28×10^{-18} cm^2. Feil *et al.*[61] separated the $C_2H_2^{2+}$ signal from CH^+. The two cross sections show different energy dependences: the double ionization has a threshold of about 45 eV, compared to about 22 eV for CH^+ produced in single ionization, and the amplitude of the maximum $C_2H_2^{2+}$ signal is 1/3 that of CH^+, see Fig. 12.

8.4. Semi-empirical analysis

The Born-Bethe approximation for total counting ionization Binary encounter Born-Bethe (BEB) model, developed by Kim and Rudd,[68] has proved to be successful in predicting total ionization cross sections for atoms and some molecules. As was discussed in detail for CH_4,[69] the observed discrepancies between the model and measured cross sections are rather to be attributed to misunderstandings in analyzing the experimental data rather than to the BEB model. Namely, for atoms it is easy to deconvolute the double ionization events, and it is not so in the case of molecules, for which almost all doubly charged ions dissociate into pairs of singly charged ions. Therefore, even counting all partial cross sections separately, the measured cross section is gross ionization (see

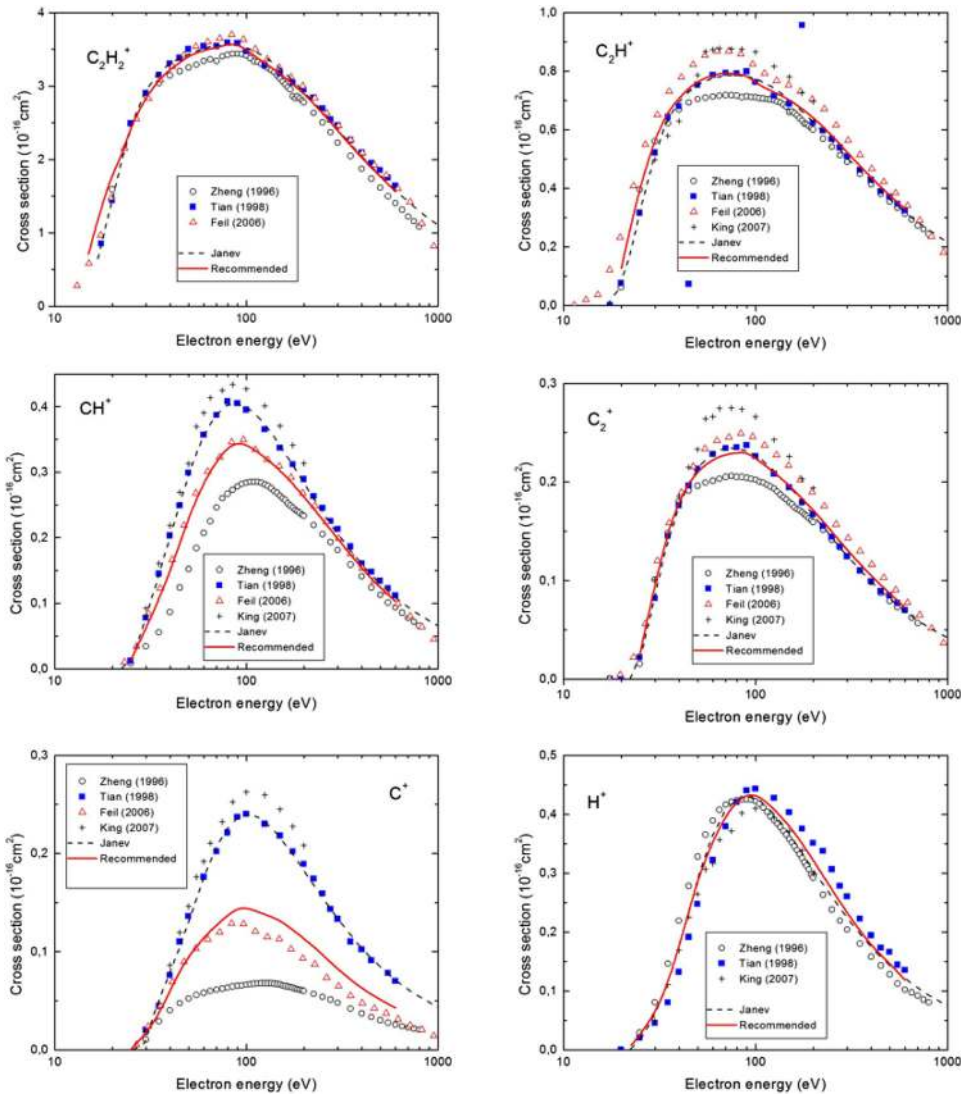

FIG. 10. Comparison of partial cross sections from different experiments. Recommended cross sections have been obtained for all ions but H^+ as non-weighted values of absolute values by Zheng and Srivastava,[59] absolute by Tien and Vidal,[56] and normalized of Feil *et al.*;[61] for H^+—as averaged values of Zheng and Srivastava and Tian and Vidal.

Ref. 23 for detailed discussion). Measurements of channel-separated ionization events, like those by King and Price,[66] allow one to obtain the counting ionization cross section, via subtracting half of the cross section for double ionization from the gross total one. This is done in Fig. 13. Note that the counting ionization cross section says how many of the impinging electrons cause ionization events; therefore this is the counting cross section to be accounted for in summing with elastic and other inelastic channels to get gross total scattering cross section, see Table 7. In the BEB model, the total (counting) ionization cross section σ is expressed as

$$\sigma = \sum_n 4\pi a_0^2 \xi_n \left(\frac{R}{I_n}\right)^2 \frac{1}{t+u_n+1} \times \left\{1 - \frac{1}{t} + \frac{\ln t}{2}\left(1 - \frac{1}{t^2}\right) - \frac{\ln t}{t+1}\right\}, \quad (3)$$

where n goes through atom subshells, ξ_n is the number of electrons on the nth subshell, I_n is the ionization energy of the nth subshell, t is the normalized kinetic energy of the incident electron $t = E/I_n$, and u_n is a normalized kinetic energy of an electron in the nth subshell, $u_n = U_n/I_n$. R is the Rydberg constant and a_0 is the Bohr radius. Unfortunately, for C_2H_2, some discrepancies exist in theoretical determinations of ionization and kinetic energies of electrons on single subshells. Kim *et al.*[68] calculated these energies using 6-311+G(d,p) basis set in the GAMESS code. Szmytkowski *et al.* used the 6-31G GTO basis set in the Hartree-Fock approximation and corrected the calculated ionization energies via outer valence Green functions using GAUSSIAN. No details of the calculated energies were given. The present energies were obtained using the wB97XD/aug-cc-pVTZ orbital basis sets in the Gaussian09 code. The theoretical energies of Kim *et al.*[68] and our present ones are compared in Table 8. As seen from the table, there are no big differences in the kinetic energies but our calculated ionization thresholds are lower (for all orbitals) than those by Kim *et al.*[68] As a consequence, our BEB integral cross sections are higher.

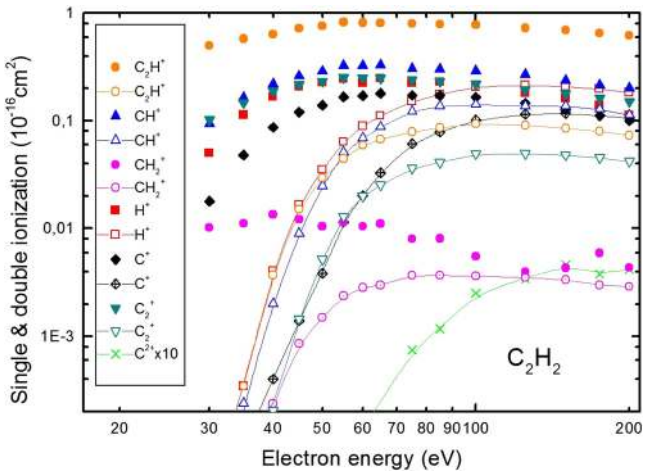

FIG. 11. Single and double-ionization partial cross sections from coincidence measurements by King and Price.[66] Their relative cross sections have been normalized to absolute $C_2H_2^+$ cross section of Tian and Vidal,[56] as it was adopted in their measurements.

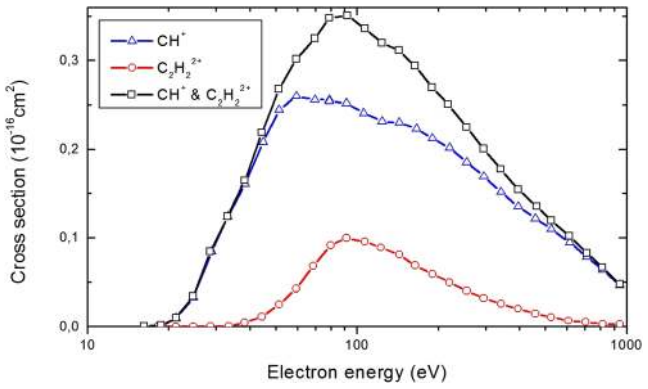

FIG. 12. Mass-resolved partial cross sections for ionization of C_2H_2 (ions with mass/charge = 13). Data adapted from Fig. 6 of Feil *et al.*[67]

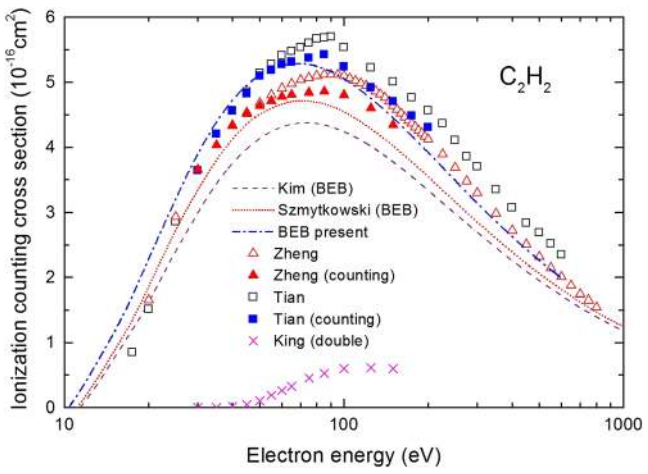

FIG. 13. Comparison of experimental total counting ionization cross sections, with three implementations of Bethe-Born binary encounter models (Kim *et al.*,[68] Szmytkowski *et al.*,[33] present), see text for details. Absolute experimental total gross ionization cross sections are from Zheng and Srivastava[59] and Tian and Vidal,[56] "King" denotes the sum of relative cross sections for the formation of dissociated ions in doubly charged ions, normalized to the $C_2H_2^+$ data of Tian and Vidal.

TABLE 8. Theoretical binding and kinetic energies of electrons on subshells in C_2H_2 used for the BEB model. See text for details

		Binding energy (eV)		Kinetic energy (eV)	
n	ξ_n	Kim	Present	Kim	Present
$1\sigma_g$	2	305.62	280.03	435.15	432.692
$1\sigma_u$	2	305.5	279.95	436.31	433.882
$2\sigma_g$	2	28.18	23.298	49.6	49.8199
$2\sigma_u$	2	20.8	17.987	32.79	33.8745
$3\sigma_g$	2	18.55	15.984	33.64	34.5002
$1\pi_u$	4	11.4[a]	10.369	28.99	30.2959

[a]Experimental value of the ionization threshold.[70]

Experimental counting of the ionization cross sections, in general, should agree with the BEB calculations. However, the discrepancies between theories do not allow us to validate the experiments in a conclusive way. Our present calculations agree well with the experiment by Tian and Vidal[56] and that by Szytkowski *et al.*[33] with the experiment by Zheng and Srivastava.[59] On the other hand, we are aware that our present model underestimates the first ionization threshold and overestimates the BEB cross section. More theoretical work is needed.

8.5. Analytical fits of partial cross sections

Numerous authors have approximated partial cross sections with analytical formulae. Shirai *et al.*[24] used the following expression with four fitting parameters a_1–a_4 for the total ionization cross section:

$$\sigma = a_1 \left[\ln\left(x + a_2\right)\right] \Big/ \left[\frac{E^2}{X}\left(1 + a_3/y\right)^{a_4}\right] \qquad (4)$$

and for partial ionization cross sections the following formula with six adjustable parameters a_1–a_6:

$$\sigma = a_1 \left(\frac{y}{R}\right)^{a_2} \Big/ \left[1 + \left(\frac{y}{a_3}\right)^{a_2+a_4} + \left(\frac{y}{a_5}\right)^{a_2+a_6}\right], \qquad (5)$$

where $x = E/I_j$ and $y = E - I_j$ is expressed in keV, $R = 0.013\,16$ keV is the Rydberg constant, and cross sections are expressed in 10^{-20} m^2. A simpler formula was used for the H^+ ion

$$\sigma = a_1 \left(\frac{y}{R}\right)^{a_2} \Big/ \left[1 + \left(\frac{y}{a_3}\right)^{a_2+a_4}\right]. \qquad (6)$$

The input cross sections were those of Tian and Vidal.[56] Parameters of the fit as given by Shirai *et al.*[24] are given in Table 9. Janev *et al.*[71] used the six-parameter expression

$$\sigma = \frac{x}{E^2}\left[b_1 \ln x + \sum_{j=2}^{6} b_j \left(1 - \frac{1}{x}\right)^{j-1}\right] 10^{-13}\,(\text{cm}^2), \qquad (7)$$

where E is expressed in eV. Parameters of their fit are given in Table 10. The parameterization by Janev *et al.*[71,72] has been used in models of thermonuclear reactors.[73] Both

TABLE 9. Analytic fit of the total and partial ionization cross sections, Eqs. (4)–(6).[24] Coefficients a_1 are in 10^{-16} cm^2 and the remaining coefficients are dimensionless

Ion	Threshold I_j (keV)	a_1	a_2	a_3	a_4	a_5	a_6
Total	1.14×10^{-2}	4.26×10^{-3}	0	4.24×10^{-2}	1.13		
$C_2H_2^+$	1.14×10^{-2}	9.55	2.59	8.81×10^{-3}	-1.97×10^{-1}	2.37×10^{-2}	9.11×10^{-1}
$C_2H_2^+$	1.65×10^{-2}	1.56	2.144	9.78×10^{-3}	-1.54×10^{-1}	2.90×10^{-2}	9.80×10^{-1}
C_2^+	1.95×10^{-2}	3.40×10^{-1}	2.83	1.10×10^{-2}	-4.05×10^{-1}	2.37×10^{-2}	9.55×10^{-1}
CH^+	2.06×10^{-2}	1.01	3.69	6.91×10^{-3}	−1.03	1.74×10^{-2}	8.76×10^{-1}
C^+	2.37×10^{-2}	7.23×10^{-2}	1.62	4.30×10^{-2}	-1.90×10^{-1}	6.30×10^{-2}	1.10
H^+	1.85×10^{-2}	6.48×10^{-2}	1.665	6.50×10^{-2}	8.38×10^{-1}		

TABLE 10. Analytic fit of the total and partial ionization cross sections, Eq. (7).[71] The a_1–a_6 coefficients are dimensionless

Process	I_j (eV)	a_1	a_2	a_3	a_4	a_5	a_6
Total	15.5	4.467	−1.317	-1.983×10^{1}	8.105×10^{1}	-1.319×10^{2}	7.876×10^{1}
$C_2H_2^+ + 2e$	15.4	4.215	−1.424	-1.570×10^{1}	6.135×10^{1}	-1.007×10^{2}	5.634×10^{1}
$C_2H^+ + H + 2e$	17.7	6.145×10^{-1}	-3.433×10^{-1}	−1.946	1.375×10^{1}	-2.479×10^{1}	1.487×10^{1}
$C_2^+ + H_2 + 2e$	22.6	-1.232×10^{-1}	1.748×10^{-1}	7.306×10^{-1}	8.969×10^{-1}	−2.714	2.449
$CH^+ + CH + 2e$	23.9	-9.656×10^{-2}	1.705×10^{-1}	1.687	−4.012	1.066×10^{1}	−5.575
$C^+ + CH_2 + 2e$	28.5	2.930×10^{-2}	1.025×10^{-1}	1.565	−6.825	1.466×10^{1}	−8.365
$H^+ + C_2H + 2e$	14.0	2.641×10^{-3}	2.024×10^{-1}	7.343×10^{-3}	−9.385	7.748	−5.168
$C_2H_2^{2+} + 3e$	50.0	5.872×10^{-2}	−9.102	5.595×10^{1}	-1.256×10^{2}	1.252×10^{2}	-4.630×10^{1}
$C_2H_2^+ + H + 3e$	70.0	1.441×10^{-4}	-6.811×10^{-4}	5.179×10^{-2}	-1.268×10^{-1}	1.215×10^{-1}	-4.342×10^{-2}

TABLE 11. Analytic fit of partial ionization cross sections, Eq. (7).[20] The a_1–a_6 coefficients are dimensionless

Process	I_j (eV)	a_1	a_2	a_3	a_4	a_5	a_6
$C_2H_2^+ + 2e$	11.40	3.732	−3.732	-8.015×10^{-1}	3.153	-1.008×10^{1}	7.289
$C_2H^+ + H + 2e$	17.30	7.970×10^{-2}	-7.970×10^{-2}	3.960	−7.247	3.705	2.815
C_2^+ (total)	18.44	2.040×10^{-3}	-2.040×10^{-3}	2.144×10^{-3}	1.629	−2.412	1.764
CH^+ (total)	20.85	9.405×10^{-13}	-9.369×10^{-13}	4.500×10^{-10}	1.051	-4.688×10^{-1}	7.147×10^{-1}
$C^+ + CH_2^+ + 3e$	28.00	1.101×10^{-9}	-1.101×10^{-9}	4.880×10^{-1}	−1.456	1.840	-6.608×10^{-1}
C^+ (total)	21.20	2.903×10^{-18}	-2.903×10^{-18}	6.158×10^{-2}	-2.106×10^{-1}	1.830	−1.234
$C_2H_2^{2+} + 3e$	36.20	1.670×10^{-1}	-1.376×10^{-1}	-2.430×10^{-2}	−1.400	9.250	−8.450

TABLE 12. Analytic fit of total and partial ionization cross sections, Eq. (8), present work. Coefficients B are the units of eV and the remaining coefficients are dimensionless

Ion	Energy range (eV)	a	b	c	d	e	B
Total	17.5–600	5.271	19.380	−79.590	141.800	−174.000	11.80
$C_2H_2^+$	17.5–600	7.274	−2.535	−31.640	109.700	−142.900	11.80
CH_2^+	20–600	−0.230	5.797	−15.400	29.340	−42.690	16.50
CH^+	25–600	−0.121	1.335	−0.616	−4.947	3.195	23.70
C_2^+	25–600	−0.044	0.839	−1.068	0.110	−1.251	23.90
C^+	30–600	0.182	−0.446	2.589	−8.380	8.996	27.20
H^+	25–600	0.272	−0.450	4.796	−20.980	24.900	21.00

Shirai *et al.* and Janev *et al.* used the experimental data of Tian and Vidal,[56] so their fits are by a few percent higher than the present recommended cross sections. Huber *et al.*[20] applied formulae Eq. (7) to partial cross sections measured by Feil *et al.*[67] Parameters of their fits are given in Table 11. In this work, the following formula, derived from the BEB approximation (as proposed in the appendix of Kim and Rudd[74]), is used to parameterize the recommended total and partial ionization cross sections:

$$\sigma = \frac{4\pi a_0^2}{t}\left[a\ln t + b\left(1-\frac{1}{t}\right) + c\frac{\ln t}{1+t} + d\frac{\ln t}{(1+t)^2} + e\frac{\ln t}{(1+t)^3}\right], \quad (8)$$

with $t = E/B$ as the normalized kinetic energy of the incident electron, and a, b, c, d, e, B—the fitting parameters (given in Table 12). As seen from Table 11, the fitting parameter B

TABLE 13. Recommended dissociative attachment cross sections for the formation of H^-, C_2^-, C_2H^-, and total dissociative electron attachment cross section from acetylene in units of 10^{-20} cm^2

Energy	H^-	Energy	H^-	Energy	C_2^-	Energy	C_2^-	Energy	C_2^-
5.58	0.02	8.16	3.63	7.17	0.01	8.46	0.69	9.75	0.04
5.68	0.05	8.26	3.25	7.22	0.02	8.51	0.62	9.8	0.03
5.78	0.01	8.36	2.54	7.27	0.02	8.56	0.57	9.85	0.03
5.88	0.01	8.46	2.27	7.32	0.04	8.61	0.49	9.9	0.04
5.98	0.02	8.56	1.93	7.37	0.06	8.66	0.5	9.95	0.05
6.08	0.02	8.66	1.59	7.42	0.07	8.71	0.41	10	0.05
6.18	0.02	8.76	1.17	7.47	0.09	8.76	0.36	10.05	0.05
6.28	0.00	8.86	0.95	7.52	0.11	8.81	0.32	10.1	0.02
6.38	0.02	8.95	0.66	7.57	0.14	8.86	0.28	10.15	0.02
6.48	0.01	9.05	0.62	7.62	0.18	8.91	0.23	10.2	0.03
6.57	0.02	9.15	0.45	7.67	0.21	8.96	0.20	10.25	0.03
6.67	0.04	9.25	0.35	7.72	0.24	9.01	0.19	10.3	0.04
6.77	0.09	9.35	0.26	7.77	0.30	9.06	0.17	10.34	0.02
6.87	0.15	9.45	0.27	7.82	0.35	9.11	0.15	10.39	0.03
6.97	0.22	9.55	0.24	7.87	0.37	9.15	0.13	10.44	0.01
7.07	0.45	9.65	0.24	7.92	0.45	9.20	0.11	10.49	0.02
7.17	0.77	9.75	0.22	7.96	0.44	9.25	0.12	10.54	0.02
7.27	1.29	9.85	0.25	8.01	0.51	9.30	0.08	10.59	0.02
7.37	1.81	9.95	0.26	8.06	0.56	9.35	0.09	10.64	0.03
7.47	2.49	10.05	0.24	8.11	0.61	9.4	0.08	10.69	0.01
7.57	3.03	10.14	0.23	8.16	0.66	9.45	0.06	10.74	0.03
7.67	3.32	10.24	0.25	8.21	0.74	9.5	0.08		
7.76	3.56	10.34	0.26	8.26	0.77	9.55	0.05		
7.86	3.81	10.44	0.23	8.31	0.79	9.6	0.04		
7.96	3.94	10.54	0.23	8.36	0.79	9.65	0.06		
8.06	3.88	10.64	0.31	8.41	0.75	9.7	0.05		

Energy	C_2H^-	Energy	C_2H^-	Energy	C_2H^-	Energy	C_2H^-	Energy	C_2H^-
1.87	0.02	3.65	1.21	5.44	0.17	7.22	0.32	9.01	0.12
1.92	0.02	3.7	1.11	5.49	0.18	7.27	0.34	9.06	0.13
1.97	0.01	3.75	1.01	5.54	0.16	7.32	0.33	9.11	0.13
2.01	0.04	3.8	0.92	5.58	0.15	7.37	0.29	9.15	0.12
2.06	0.03	3.85	0.78	5.63	0.14	7.42	0.31	9.20	0.11
2.11	0.02	3.9	0.72	5.68	0.15	7.47	0.36	9.25	0.11
2.16	0.05	3.95	0.69	5.73	0.13	7.52	0.31	9.30	0.12
2.21	0.09	4.00	0.61	5.78	0.15	7.57	0.34	9.35	0.13
2.26	0.08	4.05	0.57	5.83	0.16	7.62	0.33	9.40	0.11
2.31	0.14	4.10	0.53	5.88	0.13	7.67	0.34	9.45	0.10
2.36	0.17	4.15	0.5	5.93	0.13	7.72	0.36	9.50	0.13
2.41	0.29	4.20	0.46	5.98	0.13	7.77	0.29	9.55	0.14
2.46	0.34	4.25	0.46	6.03	0.12	7.82	0.34	9.60	0.11
2.51	0.50	4.30	0.41	6.08	0.14	7.87	0.32	9.65	0.12
2.56	0.71	4.35	0.38	6.13	0.14	7.92	0.28	9.70	0.13
2.61	1.00	4.39	0.34	6.18	0.15	7.96	0.31	9.75	0.11
2.66	1.38	4.44	0.36	6.23	0.17	8.01	0.29	9.80	0.10
2.71	1.82	4.49	0.29	6.28	0.17	8.06	0.25	9.85	0.10
2.76	2.35	4.54	0.32	6.33	0.17	8.11	0.27	9.90	0.14
2.81	2.73	4.59	0.28	6.38	0.18	8.16	0.25	9.95	0.10
2.86	3.21	4.64	0.3	6.43	0.18	8.21	0.25	10.00	0.09
2.91	3.37	4.69	0.27	6.48	0.21	8.26	0.25	10.05	0.08
2.96	3.45	4.74	0.27	6.53	0.20	8.31	0.25	10.10	0.10
3.01	3.39	4.79	0.23	6.58	0.19	8.36	0.22	10.15	0.09
3.06	3.45	4.84	0.23	6.63	0.17	8.41	0.23	10.20	0.08
3.11	3.28	4.89	0.24	6.68	0.21	8.46	0.22	10.25	0.10
3.16	3.08	4.94	0.21	6.73	0.22	8.51	0.19	10.30	0.09
3.2	2.91	4.99	0.23	6.77	0.24	8.56	0.20	10.34	0.10
3.25	2.73	5.04	0.19	6.82	0.24	8.61	0.18	10.39	0.10
3.3	2.46	5.09	0.19	6.87	0.23	8.66	0.19	10.44	0.09
3.35	2.30	5.14	0.2	6.92	0.24	8.71	0.18	10.49	0.10
3.4	2.09	5.19	0.18	6.97	0.27	8.76	0.16	10.54	0.10
3.45	1.87	5.24	0.19	7.02	0.27	8.81	0.15	10.59	0.08
3.5	1.72	5.29	0.17	7.07	0.28	8.86	0.18	10.64	0.08
3.55	1.57	5.34	0.18	7.12	0.29	8.91	0.14	10.69	0.08
3.6	1.36	5.39	0.17	7.17	0.3	8.96	0.17	10.74	0.08

reproduces roughly the ionization thresholds. Note that only four fitting parameters would be sufficient [omitting the last two terms in Eq. (8)], if the fit was performed disregarding the low-energy limit (i.e., in 30–600 eV). We stress that parameters of the fit have no direct physical interpretation: first of all, a deconvolution of partial cross sections into single, double, and triple ionization events would be needed.

9. Dissociation Cross Section

We are not aware of direct measurements of dissociation into neutrals due to electron impact. Threshold energies for the formation of neutral fragments determined in photoabsorption experiments are 7.5 eV for H/C_2H, 8.7 eV for C_2/H_2, and 10.6 eV for CH/CH pairs. Electron-impact energy loss spectra[75] show that the vibrational progression of the two triplet states ends below the dissociation threshold. On the other hand, the $\tilde{C}\,^1\Pi_u$ state, with the threshold some 0.5 eV above the C–H bond energy, is auto-dissociating (see, for example, Zhang *et al.*[76]), so we estimate that the cross section for the formation of C_2H/H pairs can be, roughly, as high as $1 - 2 \times 10^{-16}$ cm^2 at 15–20 eV.

A similar indication comes from spectroscopic measurements in low-temperature plasmas. The C_2H radical is the dominant dissociated species in low-temperature acetylene plasmas, with C, CH, and C_2 being negligible.[5] In practical applications, the C_2H radical constitutes a precursor for the formation of poly-acetylene and diamond-like films.

Note, however, that for a collision energy of 80 eV, Janev and Reiter[72] evaluated the following branching ratios: 0.51, 0.18, 0.11, 0.09, and 0.11 for (C_2 + H), (C_2 + H_2), (C_2 + 2H), (CH + CH), and (C + CH_2) dissociation channels. They proposed also the following analytical formula for the electron-collision total dissociation-into-neutrals cross section of C_2H_y species:

$$\sigma_{DE}^{tot}(C_2H_y) = 34.6\, F_2^{DE}(y)\left(1 - \frac{E_{th}}{E}\right)^3 \times \frac{1}{E}\ln(e + 0.15E)\,(10^{-16}\,\text{cm}^2), \quad (9)$$

where

$$F_2^{DE}(y) = 1.35 + 0.177\,y. \quad (10)$$

E_{th} and E are expressed in eV units, and $e = 2.171\,828\ldots$ is the base of the natural logarithm. E_{th} in Eq. (9) is the smallest of the dissociative thresholds. This formula would yield about 0.5×10^{-16} cm^2 for dissociation into neutrals of C_2H_2 at 15 eV collision energy.

10. Electron Attachment Cross Section

There are only two reports, relevant to this evaluation, on the absolute measurements of the dissociative electron attachment (DEA) cross sections for acetylene. Both are from Allan's group.[77,78] In the work of May *et al.*,[77] two mutually complementary instruments—a DEA spectrometer and a total ion collection tube—were used for measuring the cross sections. They reported two DEA peaks: C_2^- peak at 2.95 eV with a subpeak at 7.45 eV and a C_2^- peak at 8.1 eV. The 2.95 eV peak was assigned to $^2\Pi_g$ symmetry, and the 7.45 eV peak was presumed to be associated with the $^1\Delta_u$ excited electronic state of HCCH but not given an overall symmetry. Also, the 8.1 eV C_2^- band has been assigned to several Feshbach resonances with a hole in the π_u orbital and two electrons in Rydberg-like 3s and/or 3p orbitals. Later, May *et al.*[78] re-measured the ion flux with an improved apparatus. The instrument was based on the total ion-collection apparatus of their previous work.[77] Since absolute measurement of cross section requires that the ion-collection efficiency does not depend on the ion masses and their initial kinetic energies, May *et al.* improved this feature and reported a new set of DEA cross sections. In their new results, there are three DEA peaks:C_2^- peak at 8.3 eV, H^- peak at 7.9 eV, and C_2H^- peak at 3 eV. We recommend this set of

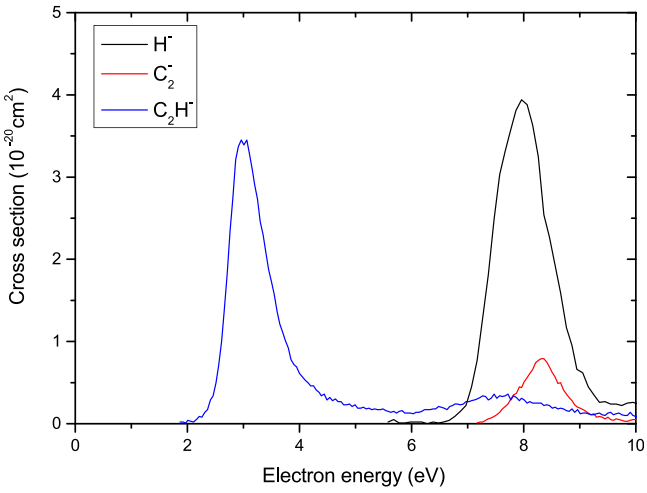

FIG. 14. Recommended cross sections for the formation of H^-, C_2^-, C_2H^-, and total dissociative electron attachment cross section from acetylene.

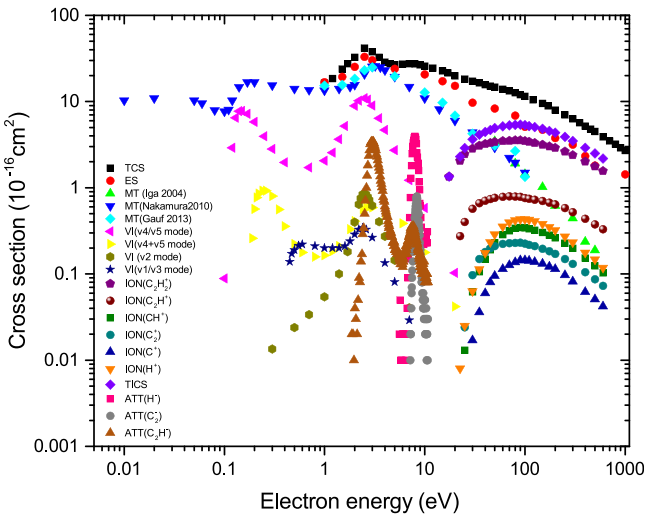

FIG. 15. The summary of cross section for electron collisions with C_2H_2. TCS—total scattering, ES—elastic scattering, MT—momentum transfer, ION—partial ionization, TICS—total ionization, VI—vibrational excitation, ATT—dissociative attachment.

DEA cross sections which are presented in Table 13 and Fig. 14. May *et al.*[78] presented the total DEA in a graphic form, which is just a numerical sum of the cross sections in Table 13. The uncertainty was estimated to be ±25%.

More recently, Szymańska *et al.*[79] investigated anion production from acetylene by electron impact. They measured the resonance peak positions of the anions produced from DEA processes: C_2^-/C_2H^- peaks at 2.5, 7.3, and 12.7 eV, and H^- peaks at 7.3 and 12.2 eV. The experimental apparatus of Szymańska *et al.* could not mass-resolve C_2^- and C_2H^-. They did not measure the DEA cross sections but only reported the relative ion yields. The positions of peaks of Szymańska *et al.*[79] investigated do not exactly match with those reported by May *et al.*[78] Furthermore, May *et al.* make no mention of the existence of the ion peaks in the higher energy region about 12 eV.

11. Summary and Future Work

We present a systematic review of the published cross sections for processes resulting from electron collisions with acetylene up to early 2016. In making recommendations, both measurements and theoretical predictions are considered, although priority is given to high quality measurements with published uncertainties where available. The summary of cross section for electron collisions with methane is given in Fig. 15. There is considerable variation in the reliability of the available data. For the total cross section, the momentum transfer cross section, and the ionization cross section, it is possible to recommend values over an extended energy range with small uncertainties, typically 5%–10%. The situation is less satisfactory for other processes. For electron impact rotational excitation, we rely on predictions from an *ab initio* calculation performed at a single, relatively high energy. Because of the high symmetry of acetylene, these cross sections are small and hard to determine empirically but experimental work on this process would be welcome. There are only a very limited number of direct experimental measurements of electron impact vibrational excitation cross sections, and these data do not agree well with each other. The more extensive theoretical treatments of this process do not give results which agree with cross sections determined from swarm experiments. We recommend the vibrational excitation cross sections determined from swarm measurements but note that this is only an indirect measurement for which it is hard to establish true uncertainties. Some new, reliable beam measurements of this process would be very helpful. Electron impact dissociation of acetylene is an important process but there are no available data for it: some measurements are needed for this process. Finally there are only sparse data available for the dissociative electron attachment process: Here we recommend using the most recent experimental data from Ref. 78 with an estimated uncertainty of 25%. We are not able to provide an extension to higher impact energies. This evaluation is the second in a series of systematic evaluations of electron collision processes for key molecular targets. Other evaluations will appear in future papers.

Acknowledgments

We thank Dr. Kamil Fedus for the analytical fits on ionization cross sections and Dr. Hee-Chol Choi in the National Fusion Research Institute for the calculation of energies for BEB analysis. One of us (G.P.K.) acknowledges greatly the hospitality at NFRI, Gunsan. V.K. acknowledges partial support from the National Science Foundation, Grant No. PHY-15-06391. This work was supported by R&D Program of "Human Resources Development and Invigoration of Education-Research-Industry Networks" through the National Fusion Research Institute of Korea (NFRI) funded by the Government funds. H.C. acknowledges the support from the research fund of Chungnam National University in 2016.

12. References

[1]H. Schobert, "Production of acetylene and acetylene-based chemicals from coal," Chem. Rev. **114**, 1743–1760 (2014).
[2]X. X. Xu, Y. J. Yang, J. Y. Sun, and J. S. Zhang, "MW-DC hybrid plasma conversion of natural gas to acetylene," Acta Chim. Sin. **63**, 625–630 (2005), available at http://sioc-journal.cn/Jwk_hxxb/EN/Y2005/V63/I7/625.
[3]S. Kado, Y. Sekine, and K. Fujimoto, "Direct synthesis of acetylene from methane by direct current pulse discharge," Chem. Commun. **1999**, 2485–2486.
[4]J. R. Fincke, R. P. Anderson, T. Hyde, B. A. Detering, R. Wright, R. L. Bewley, D. C. Haggard, and W. D. Swank, "Plasma thermal conversion of methane to acetylene," Plasma Chem. Plasma Process. **22**, 105–136 (2002).
[5]J. Benedikt, "Plasma-chemical reactions: Low pressure acetylene plasmas," J. Phys. D: Appl. Phys. **43**, 043001 (2010).
[6]J. A. Joester, M. Nakajima, N. J. Reilly, D. L. Kokkin, K. Nauta, S. H. Kable, and T. W. Schmidt, "The $d^3\Pi_g - c^3\Sigma_u^+$ band system of C_2," J. Chem. Phys. **127**, 214303 (2007).
[7]H. Ito and H. Tsudome, "Production of CH($A^2\Delta$)radicals from the dissociative excitation reaction of C_2H_2 with microwave discharge flow of Ar," Jpn. J. Appl. Phys. **54**, 06GA04 (2015).
[8]Y. M. Chen, H. Y. Zhang, Y. J. Zhu, D. Yu, Z. F. Tang, Y. Y. He, C. Y. Wu, and J. H. Wang, "A new method of fullerene production: Pyrolysis of acetylene in high-frequency thermal plasma," Mater. Sci. Eng. B **95**, 29–32 (2002).
[9]L. R. Martin, "High-quality diamonds from an acetylene mechanism," J. Mater. Sci. Lett. **12**, 246–248 (1993).
[10]M. Hundt, P. Sadler, I. Levchenko, M. Wolter, H. Kersten, and K. K. Ostrikov, "Real-time monitoring of nucleation-growth cycle of carbon nanoparticles in acetylene plasmas," J. Appl. Phys. **109**, 123305 (2011).
[11]K. De Bleecker, A. Bogaerts, and W. Goedheer, "Detailed modeling of hydrocarbon nanoparticle nucleation in acetylene discharges," Phys. Rev. E **73**, 026405 (2006).
[12]H. Okuno, J. P. Issi, and J. C. Charlier, "Catalyst assisted synthesis of carbon nanotubes using the oxy-acetylene combustion flame method," Carbon **43**, 864–866 (2005).
[13]G. Zhong, S. Hofmann, F. Yan, H. Telg, J. H. Warner, D. Eder, C. Thomsen, W. I. Milne, and J. Robertson, "Acetylene: A key growth precursor for single-walled carbon nanotube forests," J. Phys. Chem. C **113**, 17321–17325 (2009).
[14]H. Yasuda and T. Hirotsu, "Polymerization of organic-compounds in an electrodeless glow-discharge. X. Flow-rate dependence of properties of plasma polymers of acetylene and acrylonitrile," J. Appl. Polymer Sci. **21**, 3167–3177 (1977).
[15]J. Doyle, "Chemical kinetics in low pressure acetylene radio frequency glow discharges," J. Appl. Phys. **82**, 4763–4771 (1997).
[16]X. Zhang, R. Yang, J. Yang, W. Zhao, J. Zheng, W. Tian, and X. Li, "Synthesis of magnesium nanoparticles with superior hydrogen storage properties by acetylene plasma metal reaction," Int. J. Hydrogen Energy **36**, 4967–4975 (2011).
[17]L. Marcinauskas, A. Grigonis, V. Kulikauskas, and V. Valincius, "Synthesis of carbon coatings employing a plasma torch from an argon-acetylene gas mixture at reduced pressure," Vacuum **81**, 1220–1223 (2007).

[18]D. C. Bastos, A. E. Fonseca dos Santos, and R. A. Simao, "Acetylene coating on cornstarch plastics produced by cold plasma technology," Starch - Starke **66**, 267–273 (2014).
[19]Y. Peng, D. Lacroix, R. Hugon, C. Brosset, and J. Bougdira, "Experimental and theoretical investigations of absorbance spectra for edge-plasma monitoring in fusion reactors," J. Quant. Spectrosc. Radiat. Transfer **109**, 1549–1562 (2008).
[20]S. E. Huber, J. Seebacher, A. Kendl, and D. Reiter, "Assessment of hydrocarbon electron-impact ionization cross section measurements for magnetic fusion," Contrib. Plasma Phys. **51**, 931–943 (2011).
[21]M. Matsuura, A. A. Zijlstra, J. T. van Loon, I. Yamamura, A. J. Markwick, P. A. Whitelock, P. Woods, J. R. Marshall, M. W. Feast, and L. B. F. M. Waters, "Three-micron spectra of AGB stars and supergiants in nearby galaxies," Astron. Astrophys. **434**, 691–706 (2005).
[22]A. Urru, I. N. Kozin, G. Mulas, B. J. Braams, and J. Tennyson, "Rovibrational spectra of C_2H_2 based on variational nuclear motion calculations," Mol. Phys. **108**, 1973–1990 (2010).
[23]M.-Y. Song, J. S. Yoon, H. Cho, Y. Itikawa, G. P. Karwasz, V. Kokoouline, Y. Nakamura, and J. Tennyson, "Cross sections for electron collisions with methane," J. Phys. Chem. Ref. Data **44**, 023101 (2015).
[24]T. Shirai, T. Tabata, H. Tawara, and Y. Itikawa, "Analytic cross sections for electron collisions with hydrocarbons: CH_4, C_2H_6, C_2H_4, C_2H_2, C_3H_8, and C_3H_6," At. Data Nucl. Data Tables **80**, 147–204 (2002).
[25]Y. Nakamura, "Electron swarm parameters in pure C_2H_2 and in C_2H_2–Ar mixtures and electron collision cross sections for the C_2H_2 molecule," J. Phys. D: Appl. Phys. **43**, 365201 (2010).
[26]L. Andric and R. Hall, "Resonance phenomena observed in electron scattering from acetylene," J. Phys. B: At., Mol. Opt. Phys. **21**, 355 (1988).
[27]V. Krumbach, B. M. Nestmann, and S. D. Peyerimhoff, "The $^2\Pi_g$ shape resonance of the electron-acetylene scattering system: An *ab initio* treatment," J. Phys. B: At., Mol. Opt. Phys. **22**, 4001 (1989).
[28]F. Gianturco and T. Stoecklin, "Electron scattering from acetylene: Elastic integral and differential cross sections at low energies," J. Phys. B: At., Mol. Opt. Phys. **27**, 5903 (1994).
[29]S. Chourou and A. Orel, "Dissociative electron attachment to acetylene," Phys. Rev. A **77**, 042709 (2008).
[30]J. Franz, F. Gianturco, K. Baluja, J. Tennyson, R. Carey, R. Montuoro, R. Lucchese, T. Stoecklin, P. Nicholas, and T. Gibson, "Correlation–polarization effects in electron/positron scattering from acetylene: A comparison of computational models," Nucl. Instrum. Methods Phys. Res., Sect. B **266**, 425–434 (2008).
[31]M. Vinodkumar, A. Barot, and B. Antony, "Electron impact total cross section for acetylene over an extensive range of impact energies (1 ev–5000 ev)," J. Chem. Phys. **136**, 184308 (2012).
[32]E. Brüche, "Wirkungsquerschnitt und molekelbau der isosteren reihen: N_2 -$(CH)_2$ und O_2-$[(NH)_2]$-$(CH_2)_2$," Ann. Phys. **394**, 909–932 (1929).
[33]C. Szmytkowski, P. Możejko, M. Zawadzki, K. Maciag, and E. Ptasińska-Denga, "Electron-scattering cross sections for selected alkyne molecules: Measurements and calculations," Phys. Rev. A **89**, 052702 (2014).
[34]O. Sueoka and S. Mori, "Total cross section measurements for 1-400 eV positrons and electrons in C_2H_2," J. Phys. B: At., Mol. Opt. Phys. **22**, 963 (1989).
[35]R. Dressler and M. Allan, "A dissociative electron attachment, electron transmission, and electron energy-loss study of the temporary negative ion of acetylene," J. Chem. Phys. **87**, 4510–4518 (1987).
[36]S. L. Xing, Q. C. Shi, X. J. Chen, K. Z. Xu, B. X. Yang, S. L. Wu, and R. F. Feng, "Absolute total-cross-section measurements for intermediate-energy electron scattering on C_2H_2 and CO," Phys. Rev. A **51**, 414–417 (1995).
[37]W. M. Ariyasinghe and D. Powers, "Total electron scattering cross sections of CH_4, C_2H_2, C_2H_4, and C_2H_6 in the energy range 200–1400 eV," Phys. Rev. A **66**, 052716 (2002).
[38]C. Ramsauer and R. Kollath, "Über den wirkungsquerschnitt der nichtedelgasmoleküle gegenüber elektronen unterhalb 1 Volt," Ann. Phys. **396**, 91–108 (1930).
[39]E. Brüche, "Über den querschnitt von wasserstoff-und stickstoffmolekülen gegenüber langsamen elektronen," Ann. Phys. **387**, 912–946 (1927).
[40]R. E. Kennerly, "Absolute total electron scattering cross sections for N_2 between 0.5 and 50 eV," Phys. Rev. A **21**, 1876–1883 (1980).
[41]G. P. Karwasz, R. S. Brusa, and A. Zecca, *Photon and Electron Interactions with Atoms, Molecules and Ions · Interactions of Photons and Electrons with Molecules*, Landolt-Börnstein - Group I Elementary Particles, Nuclei and Atoms Vol. 17C, edited by Y. Itikawa (Springer, 2003).
[42]A. Gauf, C. Navarro, G. Balch, L. Hargreaves, M. Khakoo, C. Winstead, and V. McKoy, "Low-energy elastic electron scattering by acetylene," Phys. Rev. A **87**, 012710 (2013).
[43]M. Khakoo, T. Jayaweera, S. Wang, and S. Trajmar, "Differential electron scattering from acetylene-elastic scattering and vibrational excitation," J. Phys. B: At., Mol. Opt. Phys. **26**, 4845 (1993).
[44]I. Iga, M.-T. Lee, P. Rawat, L. Brescansin, and L. Machado, "Elastic and total cross-sections for electron scattering by acetylene in the intermediate energy range," Eur. Phys. J. D **31**, 45–51 (2004).
[45]I. Iga, I. Sanches, E. de Almeida, R. Sugohara, L. Rosani, and M.-T. Lee, "Experimental verification on the applicability of the independent-atom model (IAM) for elastic electron-molecule scattering in the intermediate-energy range," J. Electron Spectrosc. Relat. Phenom. **155**, 7–13 (2007).
[46]A. Jain, "Low energy (0.01-20 eV) electron scattering from acetylene," J. Phys. B: At., Mol. Opt. Phys. **26**, 4833 (1993).
[47]M. Herman, A. Campargue, M. El Idrissi, and J. Vander Auwera, "Vibrational spectroscopic database on acetylene, $\tilde{X}^1\Sigma_g^+$ ($^{12}C_2H_2$, $^{12}C_2D_2$, and $^{13}C_2H_2$)," J. Phys. Chem. Ref. Data **32**, 921 (2003).
[48]D. J. Gearhart, J. F. Harrison, and K. L. Hunt, "Molecular quadrupole moments of HCCH, FCCF, and ClCCCl," Int. J. Quantum Chem. **95**, 697–705 (2003).
[49]D. Thirumalai, K. Onda, and D. G. Truhlar, "Elastic scattering and rotational excitation of a polyatomic molecule by electron impact: Acetylene," J. Chem. Phys. **74**, 526–534 (1981).
[50]K.-H. Kochem, W. Sohn, K. Jung, H. Ehrhardt, and E. Chang, "Direct and resonant vibrational excitation of C_2H_2 by electron impact from 0 to 3.6 eV," J. Phys. B: At., Mol. Phys. **18**, 1253 (1985).
[51]E. N. Lassettre, A. Skerbele, M. A. Dillon, and K. J. Ross, "High resolution study of electron impact spectra at kinetic energies between 33 and 100 ev and scattering angles to 16," J. Chem. Phys. **48**, 5066–5096 (1968).
[52]S. Trajmar, J. Rice, P. Wei, and A. Kuppermann, "Triplet states of acetylene by electron impact," Chem. Phys. Lett. **1**, 703–705 (1968).
[53]S. Trajmar, J. K. Rice, and A. Kuppermann, "Electron-impact spectrometry," Adv. Chem. Phys. **18**, 15–90 (1970).
[54]G. Cooper, G. R. Burton, and C. Brion, "Absolute UV and soft X-ray photoabsorption of acetylene by high resolution dipole (e,e) spectroscopy," J. Electron Spectrosc. Relat. Phenom. **73**, 139–148 (1995).
[55]B. G. Lindsay and M. A. Mangan, *Photon and Electron Interactions with Atoms, Molecules and Ions. Subvolume C. Interactions of Photons and Electrons with Molecules*, Landolt-Börnstein - Group I: Elementary Particles, Nuclei and Atoms Vol. 17C (Springer, 2003).
[56]C. Tian and C. Vidal, "Cross sections of the electron impact dissociative ionization of CO, CH_4 and C_2H_2," J. Phys. B: At., Mol. Opt. Phys. **31**, 895 (1998).
[57]H. Straub, P. Renault, B. Lindsay, K. Smith, and R. Stebbings, "Absolute partial and total cross sections for electron-impact ionization of argon from threshold to 1000 eV," Phys. Rev. A **52**, 1115 (1995).
[58]J. T. Tate and P. T. Smith, "The efficiencies of ionization and ionization potentials of various gases under electron impact," Phys. Rev. **39**, 270–277 (1932).
[59]S. Zheng and S. K. Srivastava, "Electron-impact ionization and dissociative ionization of acetylene," J. Phys. B: At., Mol. Opt. Phys. **29**, 3235 (1996).
[60]G. Josifov, D. Lukić, D. Durić, and M. Kurepa, "Total, direct and dissociative electron impact ionization cross sections of the acetylene molecule," J. Serb. Chem. Soc. **65**, 517 (2000).
[61]S. Feil, K. Głuch, A. Bacher, S. Matt-Leubner, D. K. Böt hme, P. Scheier, and T. D. Märk, "Cross sections and ion kinetic energy analysis for the electron impact ionization of acetylene," J. Chem. Phys. **124**, 214307 (2006).
[62]A. Gaudin and R. Hagemann, "Absolute determination of the total and partial effective ionization cross-sections of helium, neon, argon, and acetylene for 100–2000 eV electrons," J. Chim. Phys. **64**, 1209–1221 (1967).
[63]R. Azria and F. Fiquet-Fayard, "Attachement électronique dissociatif sur C_2H_2 et C_2D_2," J. Phys. **33**, 663–667 (1972).
[64]N. I. Durić, Drić, D. V. Lukić, G. Josifov, M. Minić, and M. Kurepa, in *18th Summer School and International Symposium on Physics of Ionized Gases* (Institute of Physics, Novi Sad, Yugoslavia, 1996), p. 70.
[65]J. T. Tate, P. T. Smith, and A. L. Vaughan, "A mass spectrum analysis of the products of ionization by electron impact in nitrogen, acetylene, nitric oxide, cyanogen and carbon monoxide," Phys. Rev. **48**, 525–531 (1935).
[66]S. J. King and S. D. Price, "Electron ionization of acetylene," J. Chem. Phys. **127**, 174307 (2007).
[67]S. Feil, P. Sulzer, A. Mauracher, M. Beikircher, N. Wendt, A. Aleem, S. Denifl, F. Zappa, S. Matt-Leubner, A. Bacher *et al.*, "Electron impact

ionization/dissociation of molecules: Production of energetic radical ions and anions,'' J. Phys.: Conf. Ser. **86**, 012003 (2007).
[68]Y.-K. Kim, M. Ali, and M. Rudd, ''Electron-impact total ionization cross sections of CH and C_2H_2,'' J. Res. Natl. Inst. Stand. Technol. **102**, 693 (1997).
[69]G. P. Karwasz, P. Możejko, and M.-Y. Song, ''Electron-impact ionization of fluoromethanes—Review of experiments and binary-encounter models,'' Int. J. Mass Spectrom. **365-366**, 232–237 (2014).
[70]See NIST Chemistry WebBook, http://webbook.nist.gov/chemistry/.
[71]R. K. Janev, J. G. Wang, I. Murakami, and T. Kato, Technical Report NIFS-DAT 68 (NIFS, Nagoya, 2001).
[72]R. Janev and D. Reiter, ''Collision processes of $C_{2,3}H_y$ and $C_{2,3}H_y^+$ hydrocarbons with electrons and protons,'' *Phys. Plasmas* **11**, 780–829 (2004).
[73]D. Reiter, B. Küppers, and R. K. Janev, *Hydrocarbon Collision Database: Revisions, Upgrades and Extensions* (International Atomic Energy Agency, Vienna, 2014), Vol. 16, p. 102.
[74]Y.-K. Kim and M. E. Rudd, ''Binary-encounter-dipole model for electron-impact ionization,'' Phys. Rev. A **50**, 3954 (1994).
[75]D. Wilden, P. Hicks, and J. Comer, ''An electron impact energy-loss study of triplet states of acetylene,'' J. Phys. B: At., Mol. Phys. **10**, L403 (1977).
[76]Y. Zhang, K. Yuan, S. Yu, D. H. Parker, and X. Yang, ''Photodissociation dynamics of acetylene via the $\tilde{C}^2\Pi_u$ electronic state,'' J. Chem. Phys. **133**, 014307 (2010).
[77]O. May, J. Fedor, B. C. Ibănescu, and M. Allan, ''Absolute cross sections for dissociative electron attachment to acetylene and diacetylene,'' Phys. Rev. A **77**, 040701 (2008).
[78]O. May, J. Fedor, and M. Allan, ''Isotope effect in dissociative electron attachment to acetylene,'' Phys. Rev. A **80**, 012706 (2009).
[79]E. Szymańska, I. Čadež, E. Krishnakumar, and N. J. Mason, ''Electron impact induced anion production in acetylene,'' Phys. Chem. Chem. Phys. **16**, 3425–3432 (2014).